NR 2

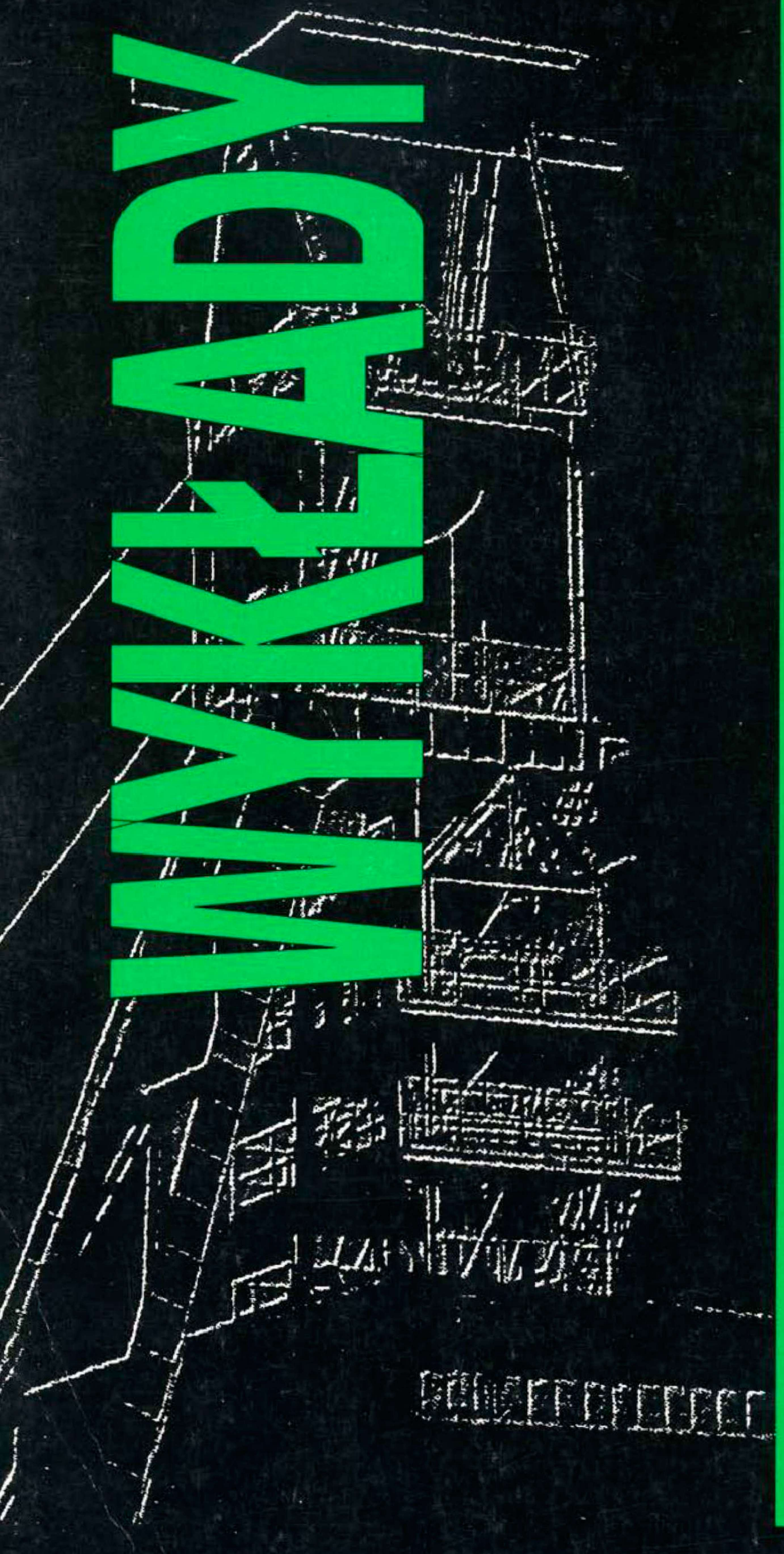

MAW

A. WAHAB KHAIR

APPLICATION OF GEOPHYSICAL METHODS IN ASSESSMENTS OF GEOLOGICAL CONDITIONS

SURFACE SUBSIDENCE PREDICTION AND PREVENTION METHODS

BIBLIOTEKA SZKOŁY EKSPLOATACJI PODZIEMNEJ

Patron
Jubileuszowego wydania
Materiałów Konferencyjnych SEP
1992-2021

KGHM
POLSKA MIEDŹ

SZKOŁA EKSPLOATACJI PODZIEMNEJ

A. WAHAB KHAIR

APPLICATION OF GEOPHYSICAL METHODS IN ASSESSMENTS OF GEOLOGICAL CONDITIONS

SURFACE SUBSIDENCE PREDICTION AND PREVENTION METHODS

Szkoła Eksploatacji Podziemnej

Jastrzębie Zdrój, 28 luty—4 marzec 1994

BIBLIOTEKA SZKOŁY EKSPLOATACJI PODZIEMNEJ

SERIA WYKŁADY NR 2

ADRES KOMITETU REDAKCYJNEGO

Szkoła Eksploatacji Podziemnej

ul. Wybickiego 7

31-261 Kraków

tel./fax (0-12) 36-12-24

fax 36-35-24

Druk publikacji wykonano na podstawie tekstów dostarczonych przez Autora

Wszelkich informacji dotyczących materiałów udziela Komitet Redakcyjny

ISBN 83-85658-22-X

Skład i druk wykonało Wydawnictwo BUS s.c.

Kraków, ul. Pawlikowskiego 14,

Wydanie I. Nakład 200 egz.

APPLICATION OF GEOPHYSICAL METHODS IN ASSESSMENTS OF GEOLOGICAL CONDITIONS

1.1 Introduction

Geophysical techniques exploit the physical properties of the rocks to investigate relatively small-scale and shallow features in the earth's crust. They have been used in the exploration for metallic minerals for several centuries and in the exploration for oil and gas since the beginning of the twentieth century.

Geophysical techniques are capable of locating and characterizing geologic structures in the coal deposits. The geologic structures that affect mining of coal include faults, folds, channel sands, shale partings and split coal, clastic dikes or clay veins, and igneous intrusions. In addition to causing roof falls, these structures may cause the coal seam being mined to decrease in thickness or even to disappear altogether. To improve the safety and profit in coal mining, it is apparent that the coal industry has to plan its operations around such geologic and human-made underground structures. Unfortunately these structures can seldom be detected by drilling boreholes. Of course, it is cheaper and quicker to perform a survey of an area using geophysical techniques than to investigate it by drilling a close grid of boreholes. However, there is no match to rotary drilling in geologically complex areas.

The geophysical techniques that may be applied to the investigation of coal deposits and to the improvement of coal mine ground control include the seismic methods, the electrical resistivity methods, and the electromagnetic methods. The physical principle, instrumentation, data acquisition and interpretation of each method will be described separately in the following sections.

1.2 Seismic Methods

The seismic methods exploit the fact that the velocity of elastic waves is different in different rocks. When elastic waves generated by a dynamite shot or any other energy source propagate through the ground, they will be reflected and refracted at the interfaces between rocks in which their velocities are different. Strictly speaking, reflections will occur only if the acoustic impedances of adjoining media are different. The acoustic

impedance is the product of the elastic wave velocity and the density of a medium. Information on the positions of the various interfaces at which the waves are reflected and refracted can be inferred from the study of the arrival times of seismic waves at a number of recording points. Seismic methods can be applied to detect faults, channel sands, no coal zones, rolls, and abandoned mine workings in coal seams.

1.2.1 Types of Seismic Waves

Two types of primary seismic waves are often observed in a seismic reflection survey. These are the body waves and the surface waves. Two distinctly different types of body waves, compressional and shear waves, are normally generated in the ground when a seismic shot is exploded or a sharp blow is imparted to the ground by any means. On the other hand, two types of surface waves are most widely observed in seismic prospecting and earthquake seismology, namely, Raleigh waves and Love waves. In addition to the body and surface waves, channel waves are also used in-seam seismic survey.

(a) Compressional or P-Waves

The particle motion associated with compressional or P-waves consists of alternating compressions and expansions during which adjacent particles of the solid are moving closer together and farther apart, respectively, in successive half cycles. The motion of the particles is always in the direction of wave propagation (Fig. 1). The relation between compressional velocity V_p and the elastic constants is given by

$$v_p = \sqrt{\frac{\lambda + 2\mu}{\rho}} \tag{1}$$

where λ and ρ are Lame's constant and shear modulus, respectively, and is density.

Alternatively,

$$v_p = \sqrt{\frac{K + (4/3)\mu}{\rho}} = \sqrt{\frac{E(1-\mu)}{\rho(1-2\mu)(1+\mu)}} \tag{2}$$

where E is Young's modulus, K is the bulk modulus, and is Poisson's ratio. Table 1 shows the typical ranges of P-wave velocities in sedimentary rocks. Note that the compressional wave velocity in Eq. 1 or 2 is the velocity in infinite medium. The compressional velocities in a bar or a thin plate, where the radius or the thickness is small compared to the wavelength, are smaller than those indicated in Eq. 1 or 2.

The compressional waves are sometimes called primary waves or simply P-waves. On reflection or refraction, a P-wave may change its character. Thus a P-wave may be reflected as a P or S wave.

(b) Shear or S-Waves

When shear deformation propagates in an elastic solid, the motion of individual particles is always perpendicular to the direction of wave propagation (Fig. 1). Shear waves are

sometimes referred to as secondary waves or simply S-waves. The velocity V_s of such waves is given by,

$$v_s = \sqrt{\frac{\mu}{\rho}} = \sqrt{\frac{E}{2}\rho(1+\mu)} \tag{3}$$

Table 1 P-wave Velocities (V_p) in Rocks

Rock Type	V_p (m/sec)
Air	330
Water	1400-1500
Alluvium, sand	300-1700
Sandstones	2000-4500
Slates and shales	2400-5000
Limestones and Dolomite	3500-6000
Rock Salt	4000-5500

The shear wave velocity is always less than the compressive wave velocity in a given medium. Similar to the P-waves, a S-wave may be reflected as a S-wave or a P-wave. As shear deformation cannot be sustained in a liquid, shear waves will not propagate in liquid materials at all. During the passage of shear waves, if the particles all move in parallel lines the wave is said to be polarized in the direction of the lines. A horizontally traveling shear wave, so polarized that the particles move in a vertical plane, is designated as a SV-wave; when its motion is in the horizontal plane, it is called a SH-wave.

(c) Rayleigh Waves

Raleigh waves travel only along the free surface of a solid material. The particle motion, always in the vertical plane, is elliptical and retrograde with respect to the direction of propagation (Fig. 2). The amplitude of the motion decreases exponentially with the depth below the surface. The speed of Raleigh waves is about nine-tenths that of shear waves in the same medium. When a low speed surface layer overlies a much thicker material in which the elastic wave velocity is higher, the Raleigh waves are sometimes called Stoneley waves, which are dispersive in nature. For very short wavelengths as compared to the layer thickness, the speed is about nine-tenths of the shear velocity in the material comprising the surface layer. For very long wavelengths, the speed is nine-tenths the shear velocity in the thicker material. Raleigh waves are the principal component of ground roll, the common designation for low velocity, low frequency surface waves that often obscure reflections on seismic records.

(d) Love Waves

Love waves are observed only when there is a low speed layer overlying a higher speed layer. The wave motion is horizontal and transverse (Fig. 2). These waves propagate by multiple reflection between the top and bottom surface of the low speed layer. The Love wave velocity is equal to that of shear waves in the low speed layer for very short wavelength and to the speed of shear waves in the higher speed layer for very long

wavelengths. Because their particle motion is always horizontal, Love waves are seldom recorded in seismic surveys, for which the detectors respond to vertical ground motion only.

(e) Channel Waves

If a seismic low velocity layer is sandwiched between two layers of higher velocities, then a large amount of energy of the body waves generated by a seismic source inside the low velocity layer will be reflected and refracted from the two interfaces and will interfere constructively to form channel (or seam or guided) waves which will propagate in two dimensions parallel to the interface. The channel wave consists of two types of waves: P-SV-waves and SH-waves. The P-SV-wave is a result of interference between P- and SV-waves and are sometimes called Raleigh waves. The SH-wave is the result of interference between horizontally polarized shear waves and is also called Love wave. Channel waves are dispersive, meaning that they have different wavelengths traveling with different velocities.

1.2.2 Seismic Sources, Detectors, and Recording Equipment

The main requirement of the seismic sources is that it should produce a short pulse that is rich in high frequencies. A few commonly used seismic sources are dynamite, weight drops, hydraulic hammers, vibraseis, and gas exploders. Among these, dynamite is the most highly concentrated source of seismic energy and is the most suitable source for high resolution seismic survey. In fact the best overall high frequency seismic source is the small explosive. Smaller explosive charges shift the peak of the spectrum to high frequencies (Fig. 3) according to the relation $f \alpha M^{-(1/3)}$ where f is frequency and M is the weight of explosive charge.

The commonest seismic detectors in use are geophones with natural frequencies of 28 Hz and 100 Hz. Geophones with high natural frequencies are used with high resolution seismic reflection survey, since the frequency response of the geophones should match the frequencies generated by the seismic sources and transmitted through the rocks. A geophone consists essentially of a coil attached to a frame placed between the poles of a bar magnet. The magnet is suspended from the frame by leaf springs and acts as an inertial element while the coil moves with the earth. The relative motion of the coil and the magnet produces an electromagnetic force (emf) proportional to the velocity of the earth's motion. This voltage is amplified and digitally recorded. Geophones may be buried in dry holes in the ground. In general, groups of geophones are used to reduce low frequency (20-80 Hz) ground roll signals. Figure 4 illustrates a common layout of surface seismic survey.

Electrical signals from the detectors are recorded digitally on magnetic tape. Nowadays most of the equipment use instantaneous floating point digital sampling. The sampling interval for signals is very important : recorders can be configured to operate at 0.25, 0.5, 1.0, 2.0, or 4.0 MS sampling. A "quick-look" analog record is also made to verify if good data are being recorded and to aid in optimizing the field procedures.

1.2.3 Data Processing and Application of Seismic Methods for Locating Geologic Anomalies in Coal

In general, the aim of computer processing or raw seismic data is to enhance the signals from features of interest and to reduce unwanted noise to a minimum. Unwanted noise include the effects of ground roll and human-made phenomena, the distortion of seismic data by velocity variations in the rocks, and differences in elevation over the survey area. The result of processing the digital data is normally a seismic record or seismogram.

In the mapping of coal, an energy source is activated to impart a seismic signal into the earth. Seismic waves travel from the input point to the coal surface which acts as a mirror, reflecting part of the waves back toward the surface. The geophones detect these reflected seismic waves and produce a small voltage representative of the received waves. These voltage pulses are recorded both in analog form and on magnetic tape which are digitally processed later. Figure 5 shows a typical seismic reflection analog record. Reflections from the sand itself may be used to determine its occurrence. The analog record alone, however, does not have the resolution required for detailed subsurface mapping. So the digital field tape is processed on a computer and a seismic record of seismogram which resembles a picture of the subsurface is reconstructed to scale.

To aid the computer processing of data and improve the analysis, a downhole velocity survey to at least the coal depth or a seismic refraction survey must be performed while on site . The velocity of the seismic wave has to be known accurately to determine the depth and character of the subsurface geology. If a deep drill hole or a well is available, a velocity survey is made in this hole to determine the seismic velocities of the layered strata. Either the well shooting or the continuous velocity log (CVL) technique will achieve this purpose. In the well shooting a shallower but nearby borehole is loaded with dynamite and detonated while a geophone records the arrival time of the waves at various depth intervals in the deep borehole. In the continuous velocity log, a sonic tool consisting of one transmitter and two receivers separated by a distance of 1 ft is operated in fluid-filled boreholes using the fluid as a coupling medium. If a well is not available, a seismic refraction survey is made to obtain approximate seismic velocities. Figure 6 shows how refraction data are collected. The seismic waves impinge on the interface at critical angle i_1, where

$$i_1 = \sin^{-1}\frac{v_1}{v_2}$$

After being critically refracted at the interface, in the lower medium they radiate energy back to the surface at the same critical angle. The first arrival time for each geophone is then plotted against the source-geophone distance as shown in Fig. 7. The velocity of layer 1 is equal to the reciprocal of the slope before the crossover distance, while the velocity of layer 2 is equal to the reciprocal of the slope after the crossover distance. This velocity information is later used to calculate the depths to each reflecting horizon. Figure 8 displays the actual results of computer data processing. In this display near surface reflections that were obtained from the coal can be seen. The heavy line over the

reflections are for facilitating interpretation. Near the left of this line the reflections are poor because the coal has disappeared. A channel sand appears near the right side of the figure. From several such lines of investigation a three-dimensional structure diagram can be constructed to reveal the channel sand patterns and other subsurface geology. This structure diagram will be very useful in optimizing mine layout and operations (Lepper and Ruskey, 1977).

Most of the seismic surveys currently being conducted underground involve the use of channel waves propagating in the coal seam to detect discontinuities in advance of mining. In the in-seam seismology work two techniques are used in the detection of discontinuities in the coal seam: the transmission method in which the distortion of the channel waves as they pass a disturbance is recorded, and, the reflection method in which the reflected waves are recorded (Jackson, 1981). Figure 9 shows the conceptual behavior of the channel waves reflected from or transmitted through certain geological discontinuities or anomalies (Suhler et al., 1978). The energy sources for in-seam seismic survey are usually small (0.1-0.2 kg) amount of permissible explosives placed in drill holes 6-10 ft deep in the center of the coal seam. These are most suitable for generating P-SV-waves. Other energy sources such as piezoceramic transducers are also used to generate SH-waves (Suhler et al., 1978). An exploder with a coupling to the seismic recorders is used to record the time when the explosion is initiated (the time break).

An experimental layout for transmission and reflection experiments on a retreating face is shown in Fig. 10 (Rueter and Schepers, 1979). Transmissions experiments are carried out by shooting between working faces or panel entries through a panel of coal. The shots are located in the headentry and the geophones in the tailentry, or vice versa. A transmission seismogram is shown in Fig. 11a. The first arrivals are P waves that have traveled through the surrounding rocks. These are followed by the S-waves and later by the channel waves. If the traveling paths of the seismic waves intersect a fault, then the channel wave will either not appear or appear in an altered form. The location of the fault can be determined by using the image reconstruction techniques. Reflection surveys are carried out by shooting from an entry or working face and putting the geophones in the same entry or face (Fig. 10). A reflection seismogram is shown in Fig. 11b. The first arrivals are the P-waves that travel through the surrounding rocks. These are followed by the so called roadway mode-dispersive waves that travel along the face or entry. The last arrival is the reflected channel wave. The reflection technique is also capable of mapping faults, channel sands, or other disturbances in coal seams.

1.3 Electrical Resistivity Methods

Electrical resistivity methods applied from the surface have been used to map the thickness and depth of coal seams and structural disturbances in the deposit and also to locate abandoned mine workings. They can also be used to predict roof falls (Burdick, 1982). The methods may be used from the surface or underground as well as in drill holes.

1.3.1 Principles of Electrical Resistivity Methods

The principle of the method is that a direct or low frequency alternating current is introduced into the ground by means of two current electrodes which may be iron stakes or suitably arranged bare wire connected to the terminals of a source of emf. The resulting potential distribution in the ground is mapped by two potential probes, again iron stakes or nonpolarizable electrodes. The equipment for making these measurements can be as simple as using a battery for injecting current into the ground and a sensitive voltmeter to measure the resulting potential, or as complicated as the U.S. Bureau of Mines' prototype Automatic Resistivity System (Burdick, 1982). There are four different electrode configurations for electrical resistivity survey. The two resistivity methods most commonly used for mining applications are the Wenner method (Fig. 12) and the pole-dipole method (Fig. 13).

The Wenner method is used in two ways. In the first method the electrode spacing is held constant, and the entire array is traversed across the ground surface. This results in looking at a large area to a constant depth. This constant-depth traverse may be used to look for geologic faults, shallow voids, lithologic contacts, and so on. The second method is to maintain a constant center to the electrode array and incrementally increase the electrode spacings. This results in a deeper and deeper measurement depth with an associated larger and larger measurement volume. From these data sounding curves may be constructed for interpretation of the earth material at depth (Burdick, 1982). The pole-dipole method used several current electrodes, one at a time, near the measurement site and the other at effective infinity (5 to 10 times the largest separation between the other current electrode and the potential electrodes) as shown in Fig. 14. The potential electrodes are moved as a pair with predetermined separation between them. This method may be used for performing either a constant depth traverse or a depth-sounding, but in practice a combination of the two is run to obtain a cross-sectional view of the earth below the array position.

The resistivity methods do not measure geologic faults or abandoned mine workings directly, but, simply measure the changes in the volume resistivity caused by their presence. A dense, competent rock with few microfractures will contain relatively less moisture than a porous rock and will normally exhibit a much higher resistance to the passage of an electrical current than will the more porous rock.

1.3.2 Use of Electrical Resistivity Methods to Locate Geologic Faults

Figure 14 shows the principle of using electrical resistivity to locate faults. A fault may be detected either when it serves as a drain for surface moisture resulting in a somewhat drier zone around the fault, or, when it contains more moisture than the surrounding area. A third possibility exists when a fault has shown sufficient vertical displacement to bring dissimilar lithologies close to the surface to be within the measurement zone (Burdick, 1982).

1.3.3 Use of Electrical Resistivity Methods for Detection of Abandoned Mines in Proximity to Current Mining Activities

The premise made for the application of electrical resistivity for detecting abandoned mines is that old workings, whether air or water filled, will show a different apparent resistivity than the surrounding earth material. Figure 15 shows the use of the pole-dipole method to detect a void (Burdick, 1982). The lines A, B, and C would be run simultaneously with the automated resistivity system. From the points where the void was detected on A, B, and C, the void may be located in a manner similar to that shown in Fig. 13.

Peters and Burdick (1983) reported a high resolution earth resistivity system for detecting abandoned coal mine workings. Figure 16 shows the conceptual diagram of the pole-dipole earth resistivity data acquisition system. Magnetic tapes recorded in the field are processed to yield a cross-sectional image of resistivity anomalies underlying the survey line. Resistance anomalies detected along the survey lines can be plotted in two forms of image patterns, gray shadings or contours. The contours in a contour plot represent equal correlation coefficients for detected anomalies. The darkest intensity in a shade-of-gray plot depicts the highest probable location and depth of a resistivity anomaly.

1.3.4 Use of Electrical Resistivity Methods to predict Roof Falls

The assumption made in the case of roof falls is that the delamination or fracturing cracks preceding a fall will cause a change in volume apparent resistivity, which can be interpreted as an indication of failure (Fig. 17). This figure shows how cracks caused by delamination or other fracturing in the roof can affect the resistivity measurements. The plot of resistivity versus time shows the normal scatter of data points preceding failure and the much greater change in values as cracking starts and progresses (Burdick, 1982).

1.4 Electromagnetic Methods

The electromagnetic methods discussed here will be confined to the use of electromagnetic radiation as a hazard detection method that measures electrical and magnetic properties of the ground. In order to provide adequate penetration and resolution in coal, frequencies of electromagnetic radiation between 15 and 500 Mhz are normally used. This translates to wavelengths between 66 and 2 ft. in free space and 22 to 0.66 ft. in coal having a velocity of propagation approximately one-third that of free space. With this band of frequency the electromagnetic methods can be used to detect various targets in coal seams at distances of 50 ft. or more.

Electromagnetic radiation may be used in a number of ways in the examination of coal deposits. The short-pulse radar method, in which reflections from small disturbances are detected, has been tested in underground coal mines. The radar may have a range of about 150 ft. in coal under good conditions and is particularly effective at detecting small features such as water-filled tunnels, abandoned oil and gas wells, clay veins, and sand lenses in

the coal deposits. The high frequency continuous wave method uses continuous electromagnetic waves, usually transmitted between boreholes in a coal seam. Geological or human-made disturbances cause changes in the phase and amplitude of the transmitted curves. Analysis of these changes allows the location of disturbances to be determined. In the synthetic pulse method hundreds of discrete frequencies are transmitted and recorded. By processing the return signals, pulselike data can be obtained. Applications of the synthetic pulse method are very similar to those of the short-pulse radar method, except that the range of the former is longer. Another electromagnetic method that has been used in the examination of coal deposits is the FM-CW method. This method can be used to detect the interface between a coal seam and the surrounding rocks, in addition to disturbances in the seam.

The Radio Imaging Method (RIM) represents another recently developed electromagnetic method. It is an electromagnetic (EM) wave process that consists of in-mine and surface survey techniques (Fry et al., 1985). Both techniques are used in underground coal mines to detect faults, interbedding, sandstone channels, and thinning coal.

1.4.1 Principles of the Electromagnetic Methods

The underlying principle for electromagnetic methods is to determine and measure the effect the earth material has on the electromagnetic radiation as it passes through the ground. The major physical parameters affecting the propagation are the frequencies of the waves, the dielectric constant, and the relative permeability of the earth material. The dielectric constant affects the velocity at which the waves travel but not their range. On the other hand, electrical resistivity of a material affects the range of an electromagnetic wave propagation. Higher dielectric constant means lower velocity. Lower resistivity means higher absorption of energy and shorter range. Coal has low dielectric constant (2-4 electrostatic unit). The dielectric constants are 6-16 esu for hard rocks and 40-50 esu for wet soils and clays. Water has a high dielectric constant of around 80 but a low resistivity.

Whenever there is a change in either the dielectric constant or the relative permeability, the electromagnetic waves will be reflected or refracted with associated changes in velocity, amplitude, and polarization taking place for a wave of a given frequency. It is these changes that are measured, and with general geological knowledge of an area, an interpretation can normally be made by correlating a given wave propagation change to a probable geological feature (Leckenby, 1982).

Most of the methods are used in either a reflection (radar) mode or a transillumination (one-way) mode. Figure 18 illustrates the two modes; in this case the anomaly, representative of an abandoned mine, has a different electrical property than the surrounding rock material. This change causes reflection and refraction to occur. The reflection, the echo, or the refracted wave is received via an antenna and is recorded. In the reflection mode, a surface, an air wave, and an echo are normally received (Leckenby, 1982).

1.4.2 The Short-Pulse Radar Method

The short-pulse radar method can be applied from the ground surface, a borehole, or underground openings in a mine. The method of detection is usually done by making voltage versus time measurements. The measured voltage is then recorded either on digital or analog tape. In the radar mode the anomaly is detected by receiving the echo of the transmitted wide-frequency band pulses at a delayed time (Fig. 19). For the one-way mode the signal will arrive at a different time and amplitude than what would be expected if there were no anomaly; thus an anomaly can be detected. The short-pulse radar method can also be used to locate clay veins, fracture zones, and dry and wet mine voids (Fowler, 1981).

1.4.3 The Continuous Wave Method

In the continuous wave method a high frequency continuous wave is transmitted into the ground. The technique is normally used in a transillumination mode, mainly from cross-borehole surveys. A measurement of the amplitude and phase of the received signal is made and usually reinforced to the transmitted signal (Fig. 20). In the one-way mode an anomaly can be inferred from the arrival time and amplitude of the waves received.

1.4.4 The Synthetic Pulse Method

The synthetic pulse method is an attempt to take advantage of the positive points from the continuous wave and short-pulse methods. In this method, waves of hundreds of discrete frequencies are transmitted and recorded. Otherwise, this method is somewhat similar to the continuous wave method. The synthetic pulse method can be used in a radar mode, and it is capable of doubling the effective probing range of the short-pulse method.

1.4.5 FM-CW Methods

Frequency modulated continuous waves may be used to measure the thickness of a coal layer in the roof of a mine roadway. The technique can be applied to control the cutting horizon of a continuous miner. In this method a microwave signal generator transmits waves that vary continuously in frequency, commonly from 2 to 6 GHz, and these are reflected back. The waves reflected from a target such as an air-coal or coal-shale interface travel back to a mixer. There will be a difference in frequencies between the waves currently being transmitted and those being received: the frequency difference will be proportional to the distance to the target (Jackson, 1981). The FM-CW technique can also be used to detect small disturbances in the coal seam.

1.4.6 The Radio Imaging Method (RIM)

In the Radio Imaging Method, in-mine and surface surveys employ electromagnetic waves that propagate along straight paths in the coal (Fry et al., 1985). As the RIM signal travels along a ray path, it loses energy and is attenuated. The amount of energy loss per unit path length depends upon the coal seam thickness and type of surrounding roof and

floor rock. A reading of the signal level is taken at the end of the ray path at the receiver location. This reading is used to determine the attenuation rate of the signal along the path. The signal level data is compiled and analyzed through computerized algorithms which construct images of any anomaly present. This graphical depiction of the coal seam provides a basis for further geological interpretation. This method has been successfully applied to locate sandstone channels that cut into coal seam in advance of the coal faces (Fry et al., 1985).

REFERENCES

Peng, S. S., 1986., Coal Mine Ground Control, Second Edition, John Wiley and Sons, New York, pp. 142-165.

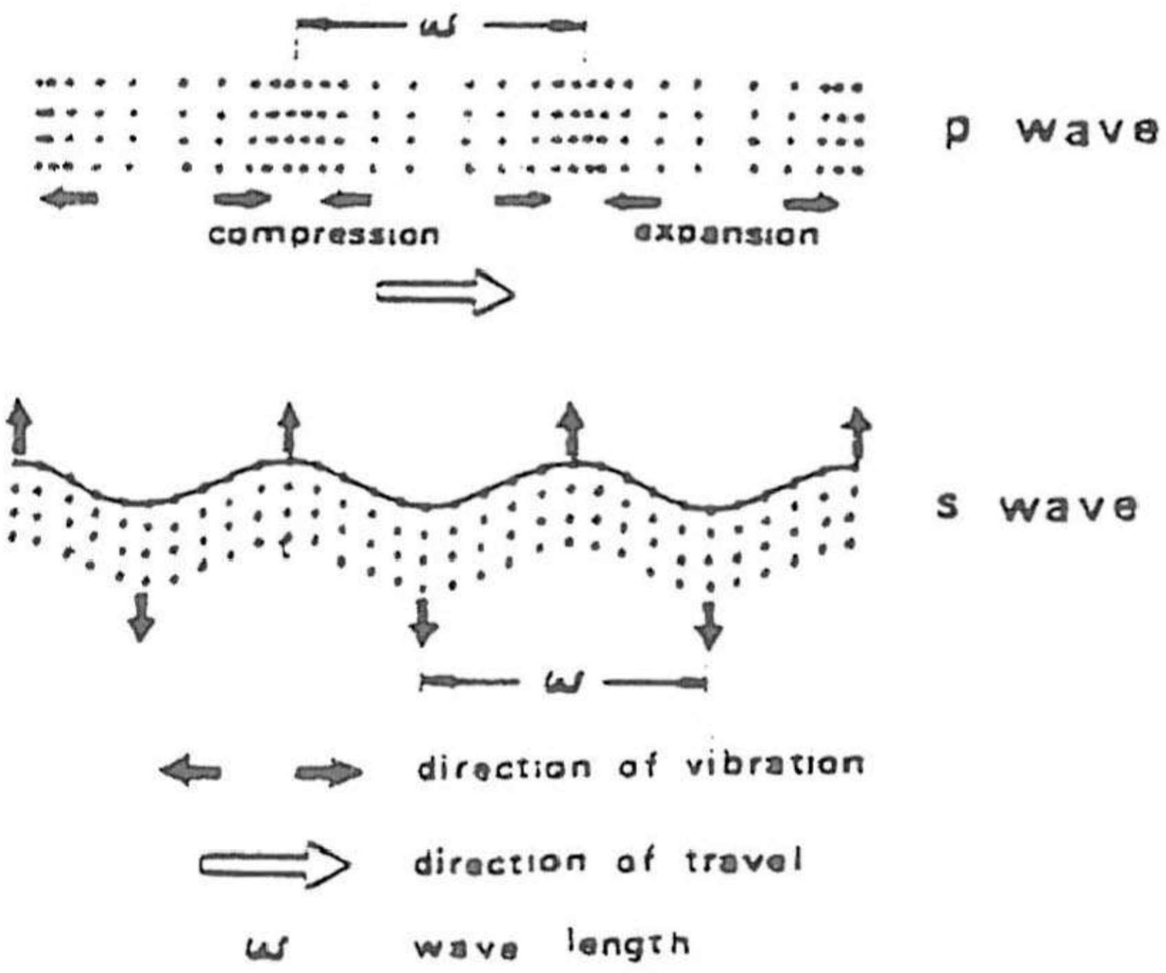

Fig. 1 Schematic diagram showing directions of particle vibrations in P and S waves.

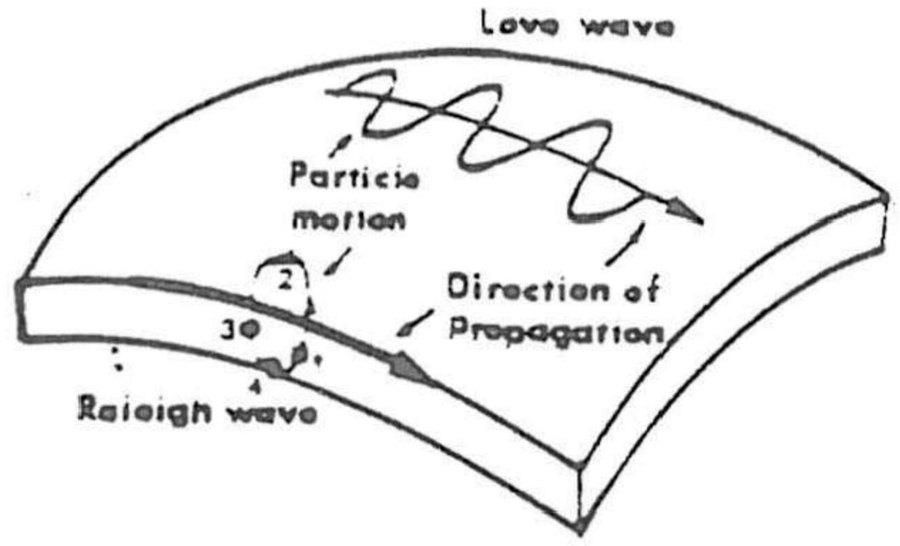

Fig. 2 Schematic diagram showing directions of particle vibrations in Raleigh and Love waves.

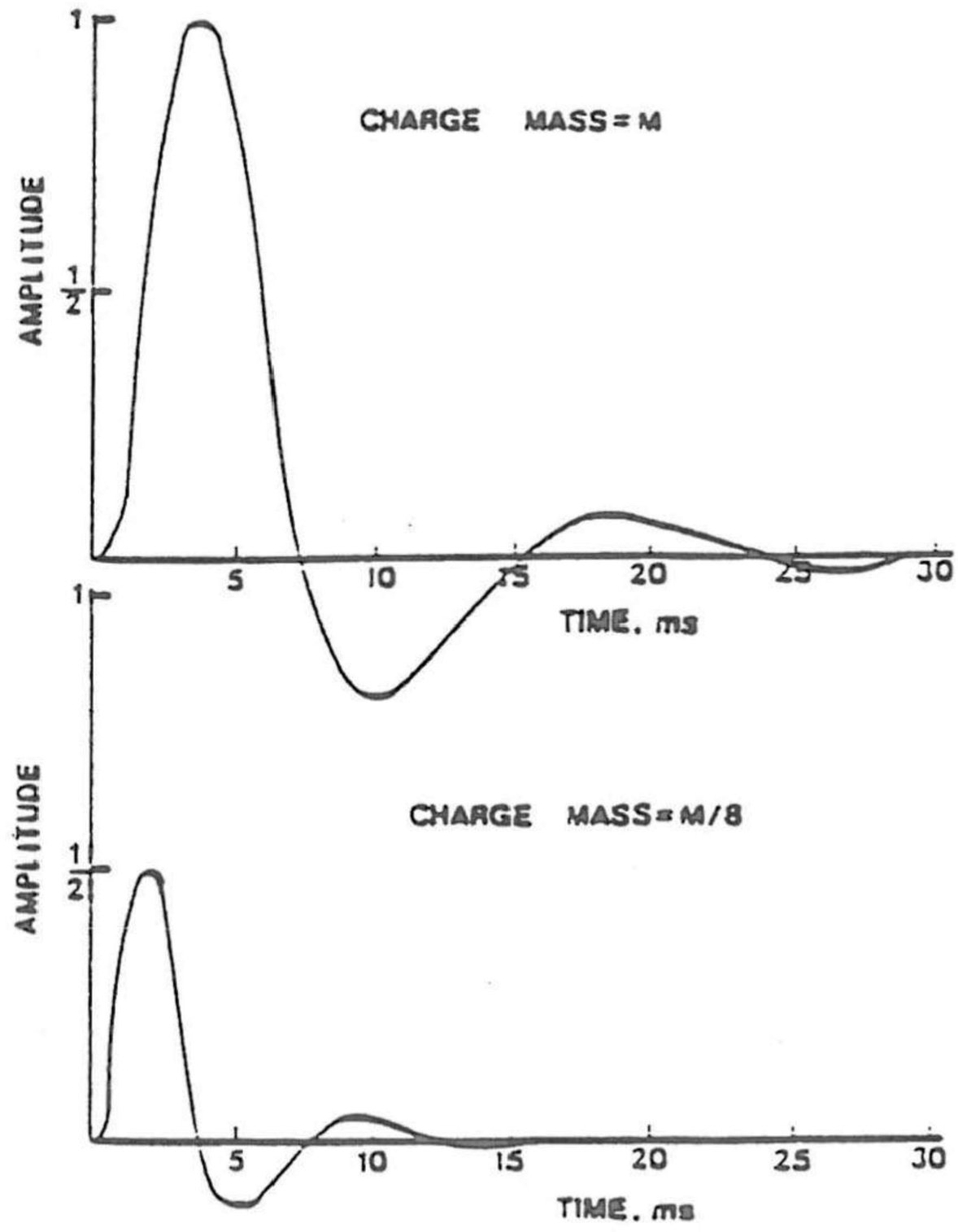

Fig. 3 Effect of reducing the mass of the charge on signal period and amplitude (Ziolkowski, 1979; Ziolkowski and Lerwill, 1979).

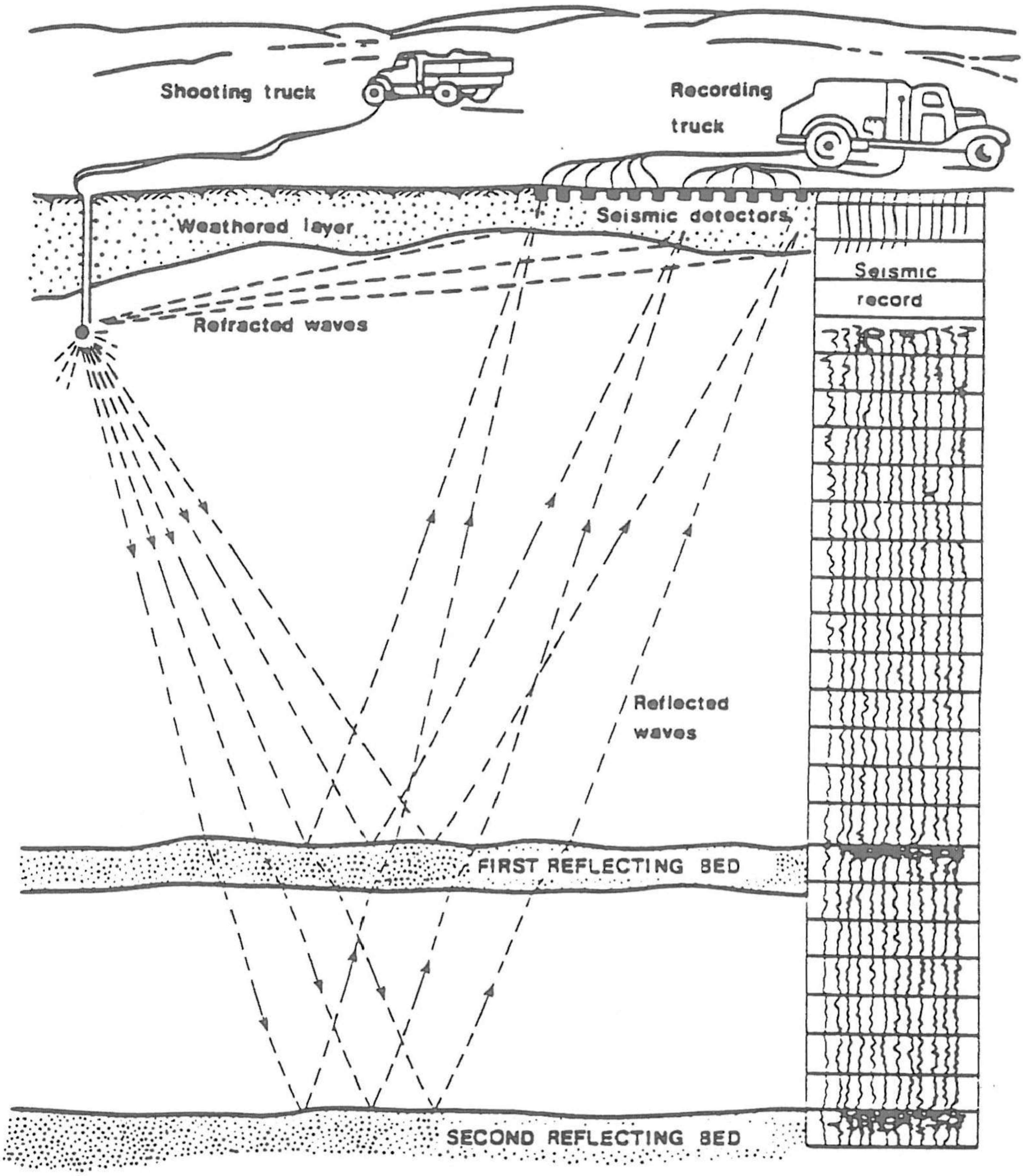

Fig. 4 Layout of surface seismic survey (Daly and Hagemann, 1976).

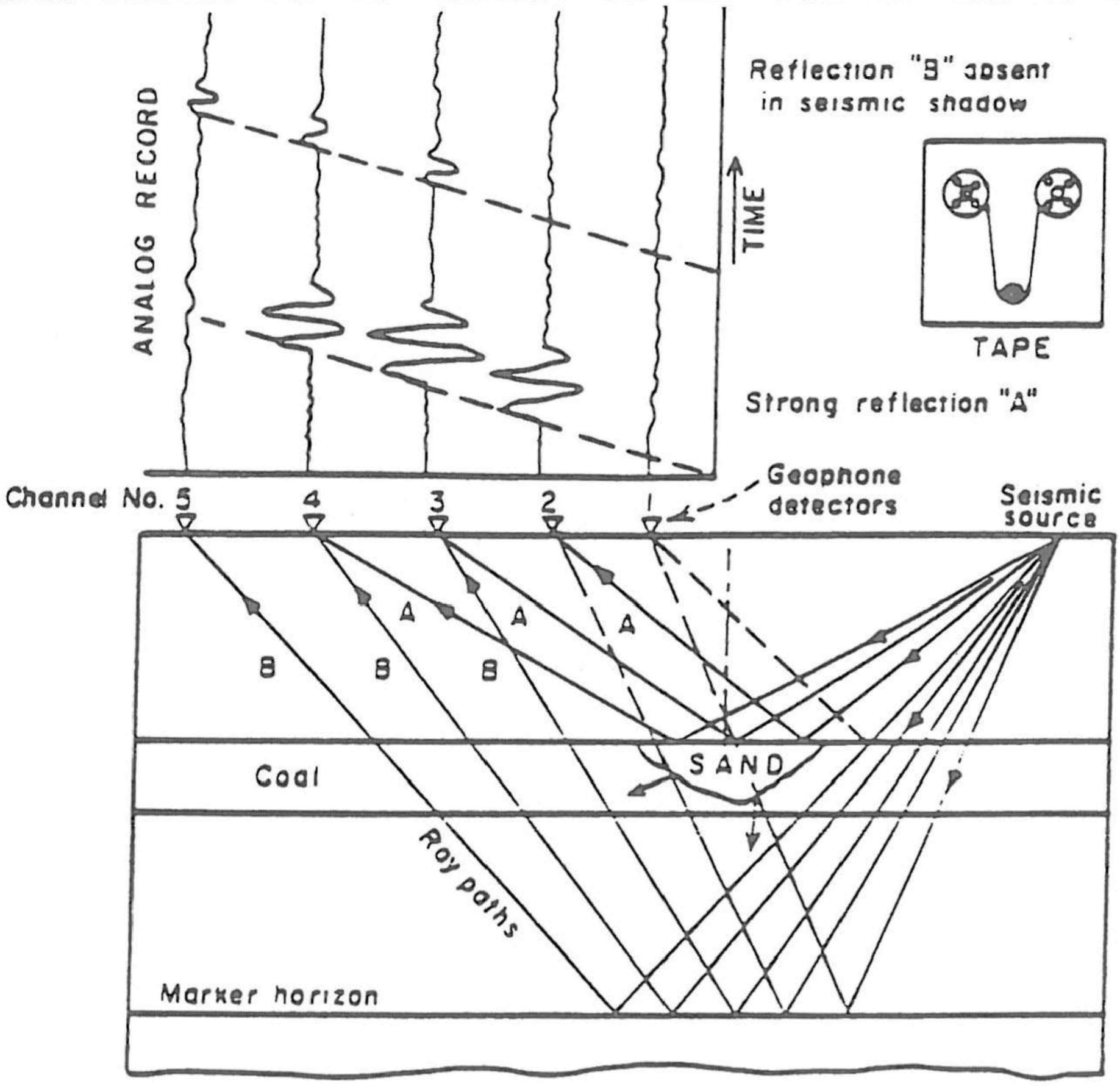

Fig. 5 Creation of a seismic reflection analog record; data also go to a digital magnetic tape. This is so-called „quick-look" record (Lepper and Ruskey, 1977).

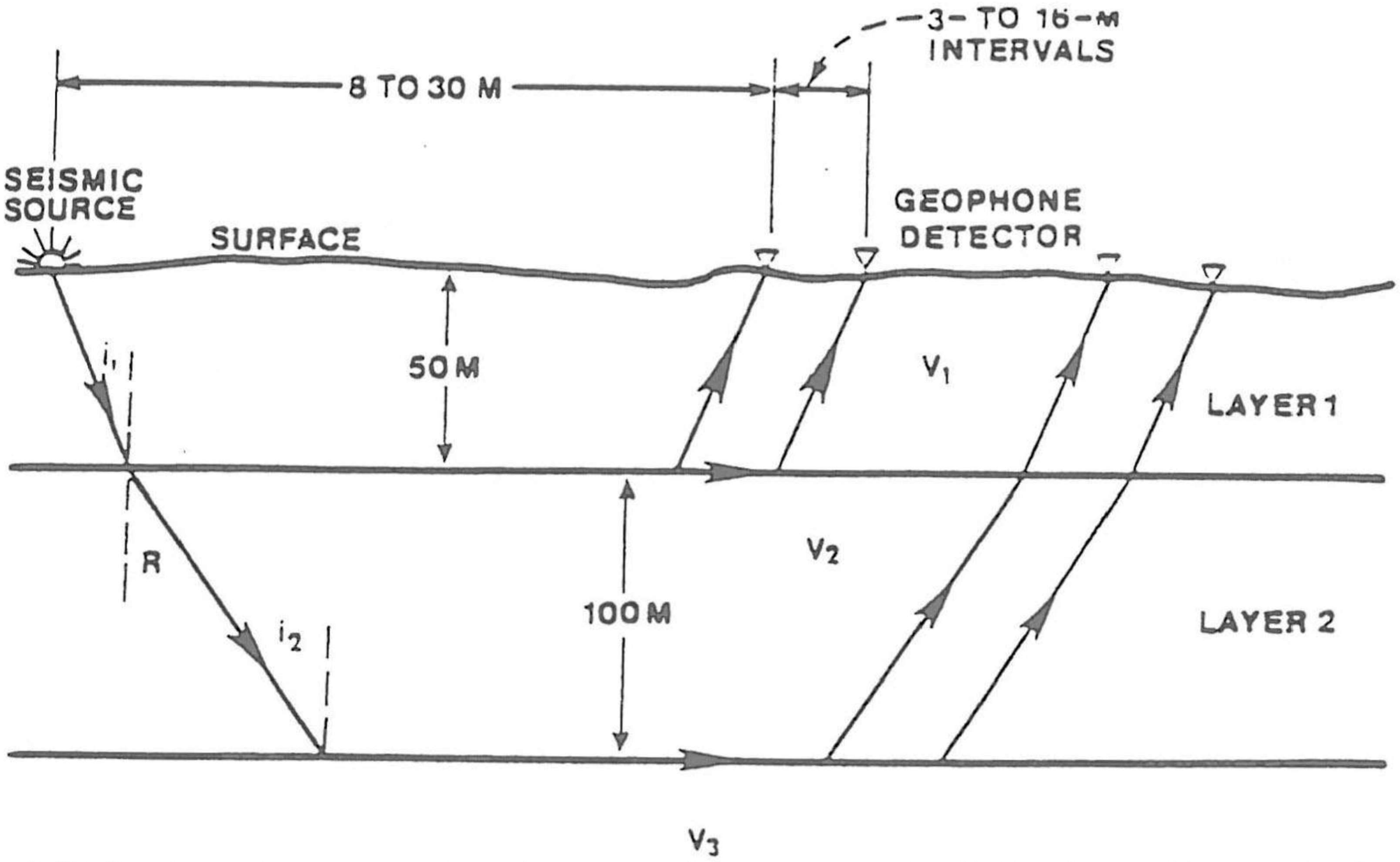

Fig. 6 Refraction seismic procedure showing various energy paths. Refraction studies may be done before or after reflection surveys (Lepper and Ruskey, 1977).

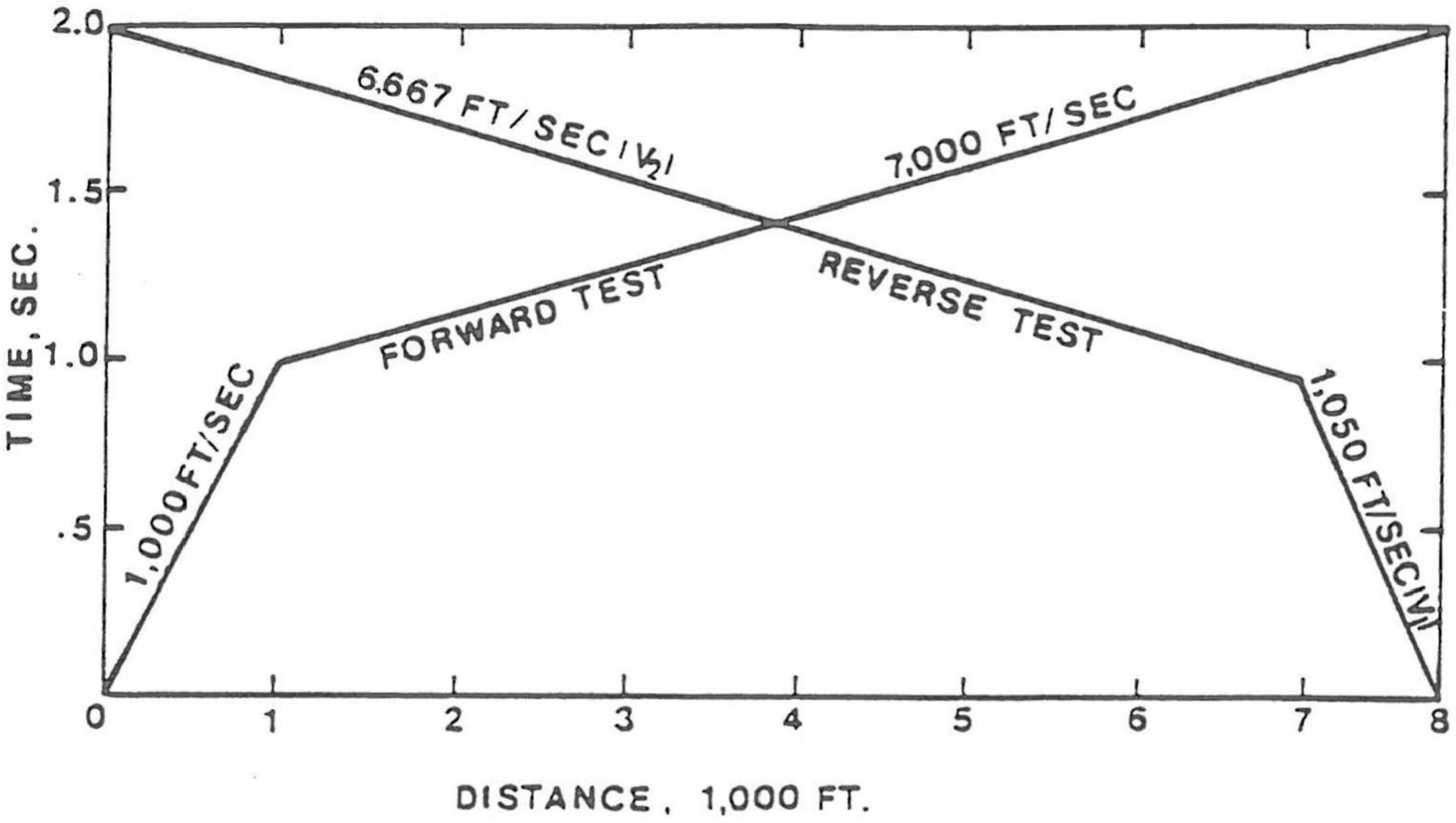

Fig. 7 Time-distance plot, shot from both ends of line (refraction method). Data are used to find depths to each reflecting horizon (Lepper and Ruskey, 1977).

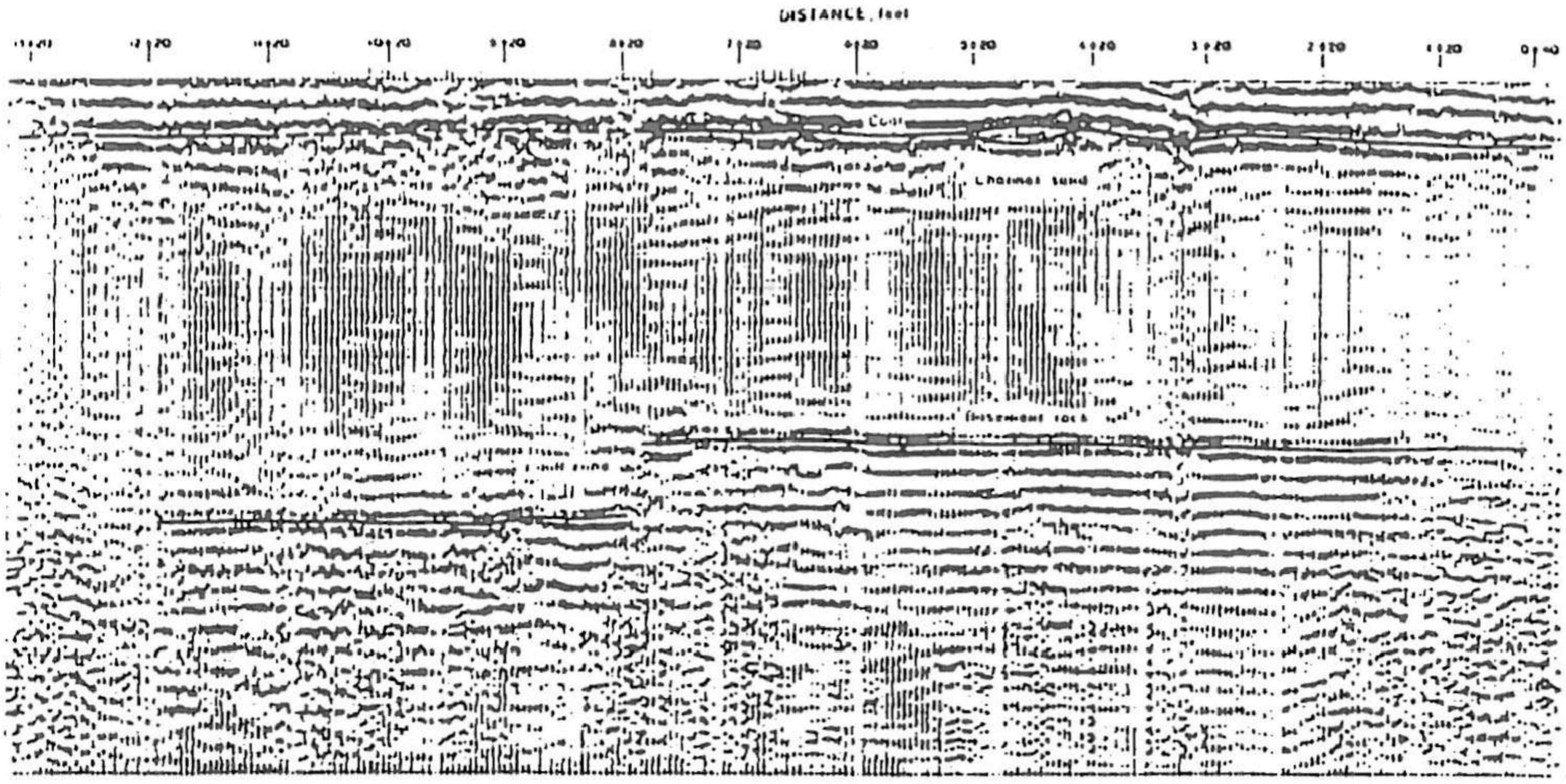

Fig. 8 When a seismic line is completed, data on the magnetic tape are processed by a computer to yield this type of diagram (Lepper and Ruskey, 1977).

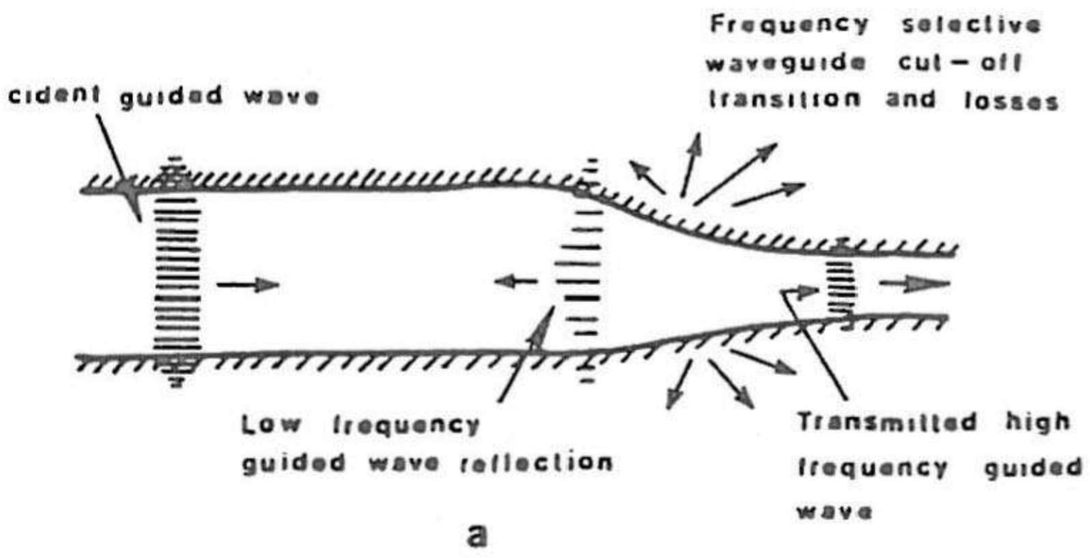

Fig. 9 Conceptual behavior of channel waves on encountering *(a)* a coal seam pinchout, *(b)* a channel sand cutout *(c and d)* faults with throws less than and greater than seam thickness (Suhler et al., 1978).

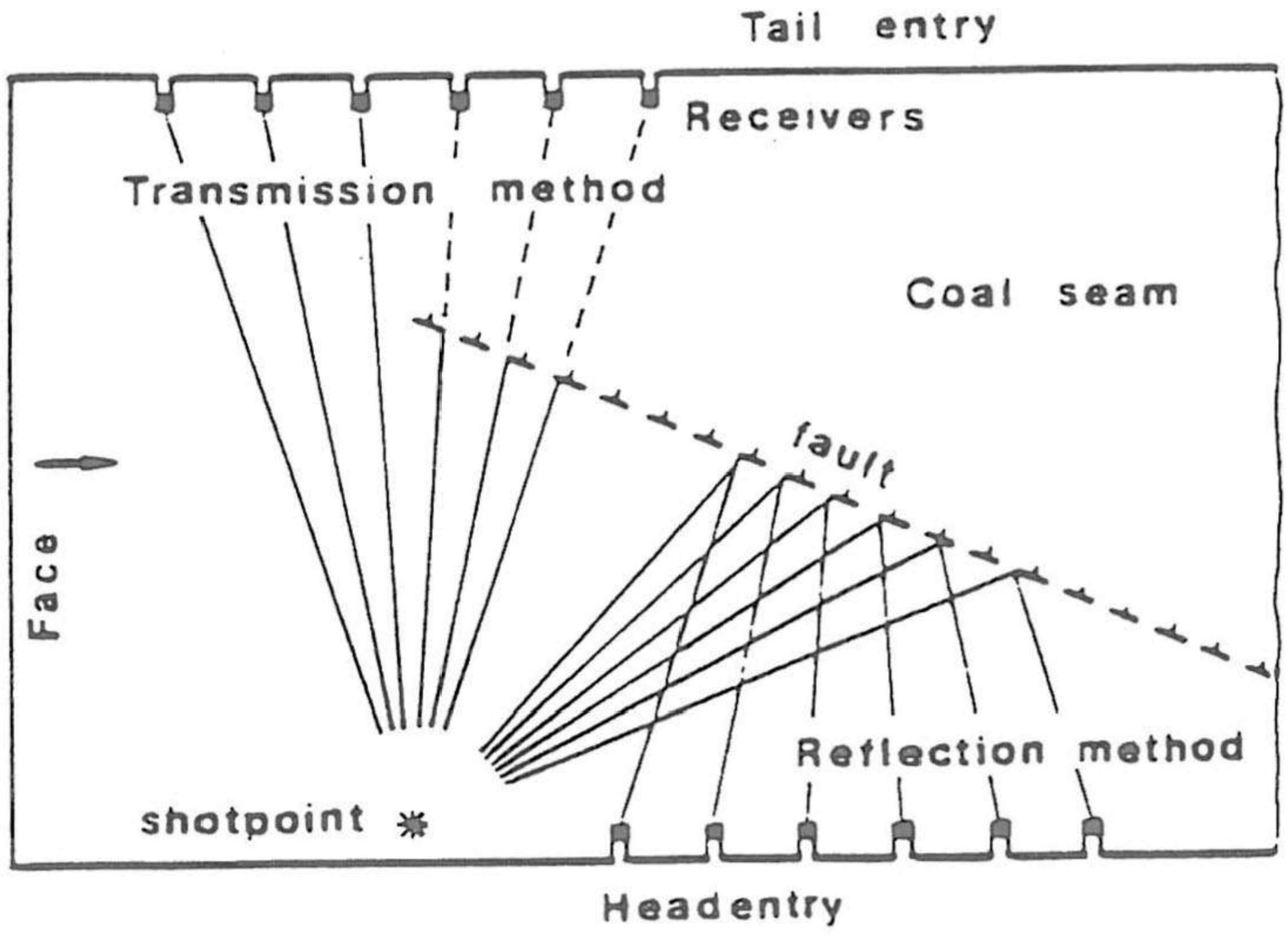

Fig. 10 Layout of shots and geophones for transmission and reflection surveys (Rueter and Schepers, 1979).

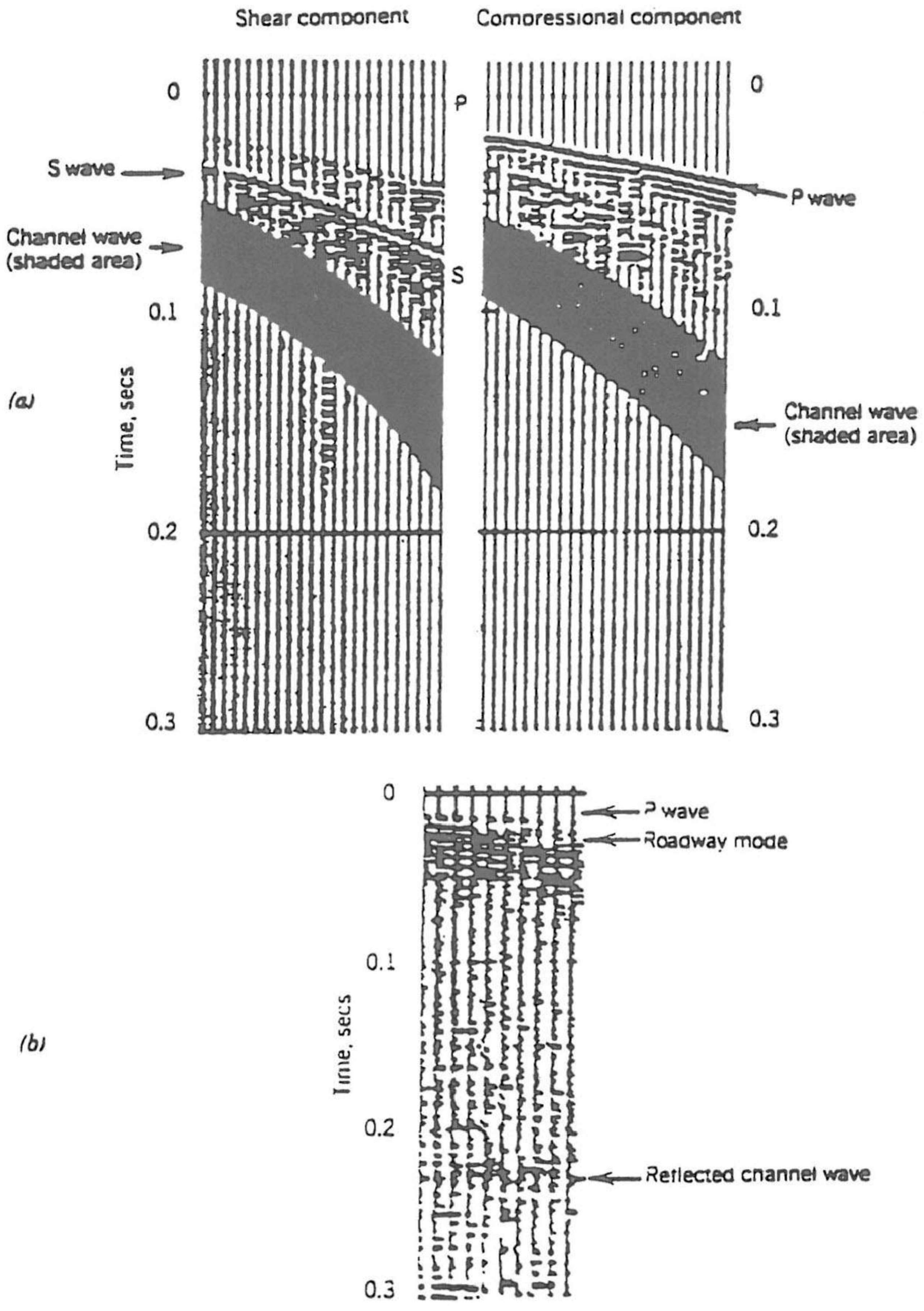

Fig. 11 Seismic records from in-seam seismic surveys *(a)* transmission survey, *(b)* reflection survey (Prakla-Seismos GmbH, 1980).

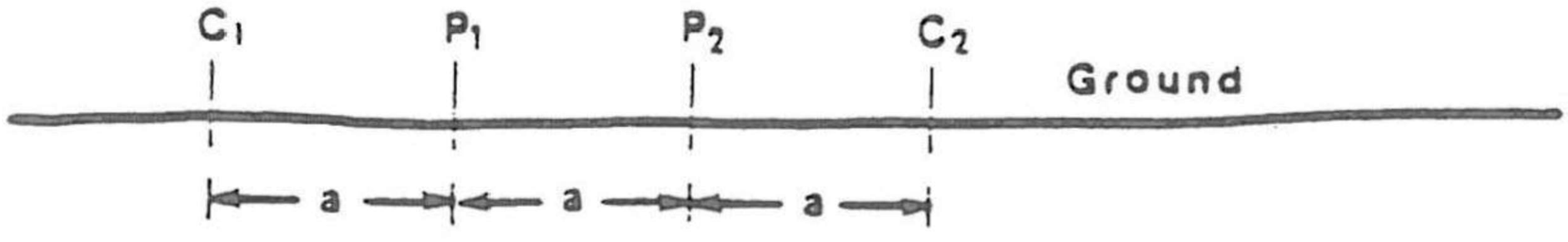

$C_1 - C_2$ Current injection electrodes

$P_1 - P_2$ Potential measument electrodes

a Electrode spacing

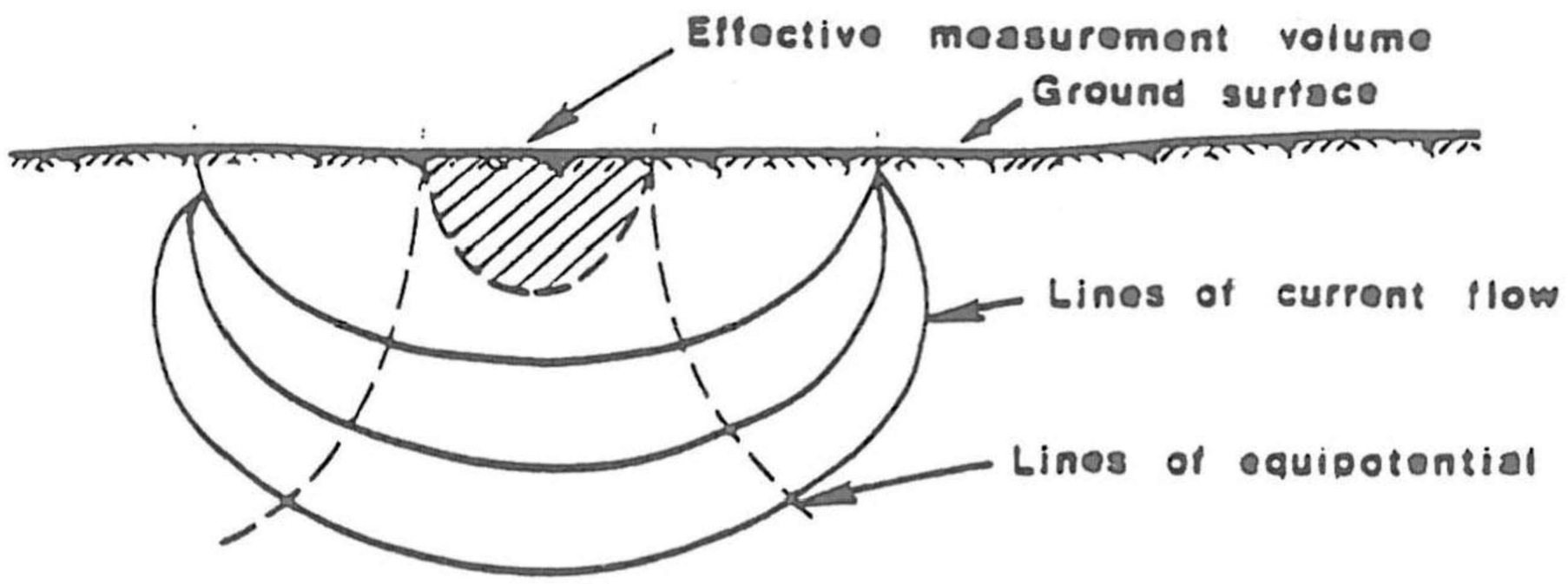

Fig. 12 Approximate current and potential fields for Wenner array (Burdick, 1982).

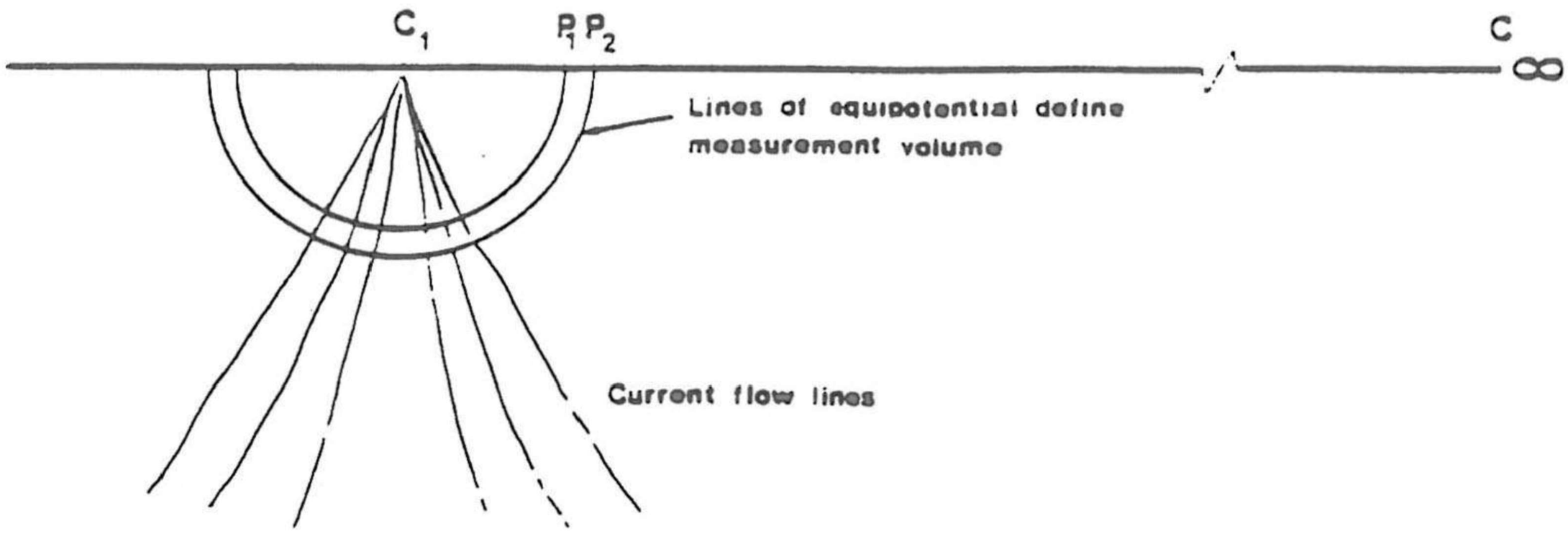

Fig. 13 Approximate current and potential fields for pole-dipole (Bristow) method (Burdick, 1982).

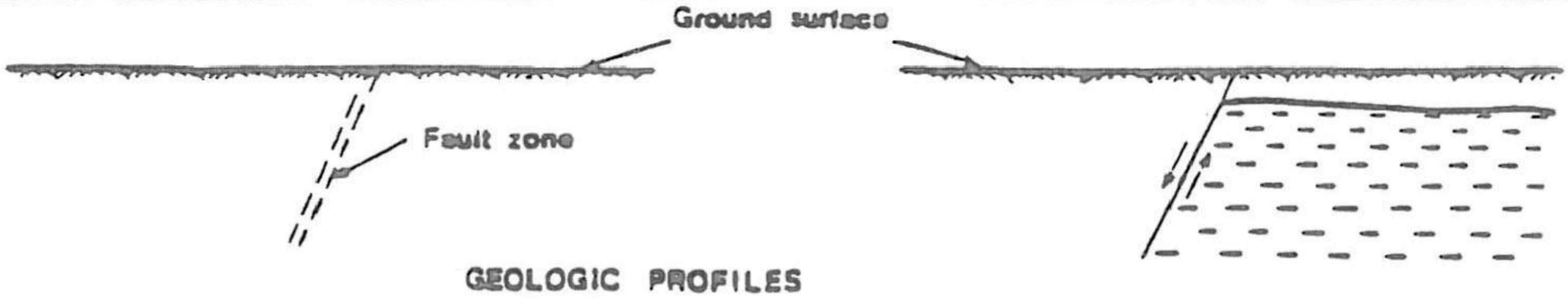

Fig. 14 Use of resistivity to detect faults (Burdick, 1982).

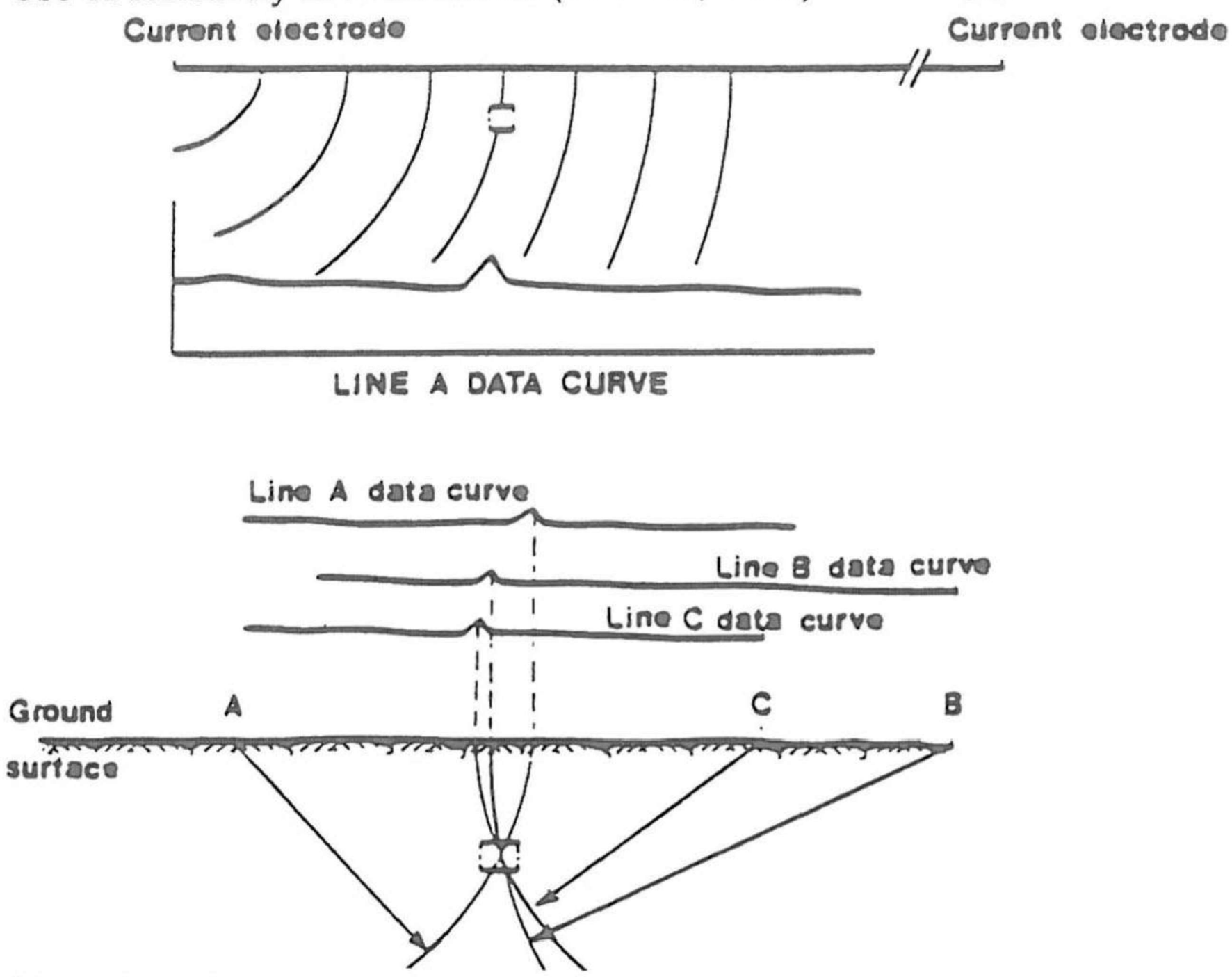

Fig. 15 Void detection with pole-dipole method (Burdick, 1982)

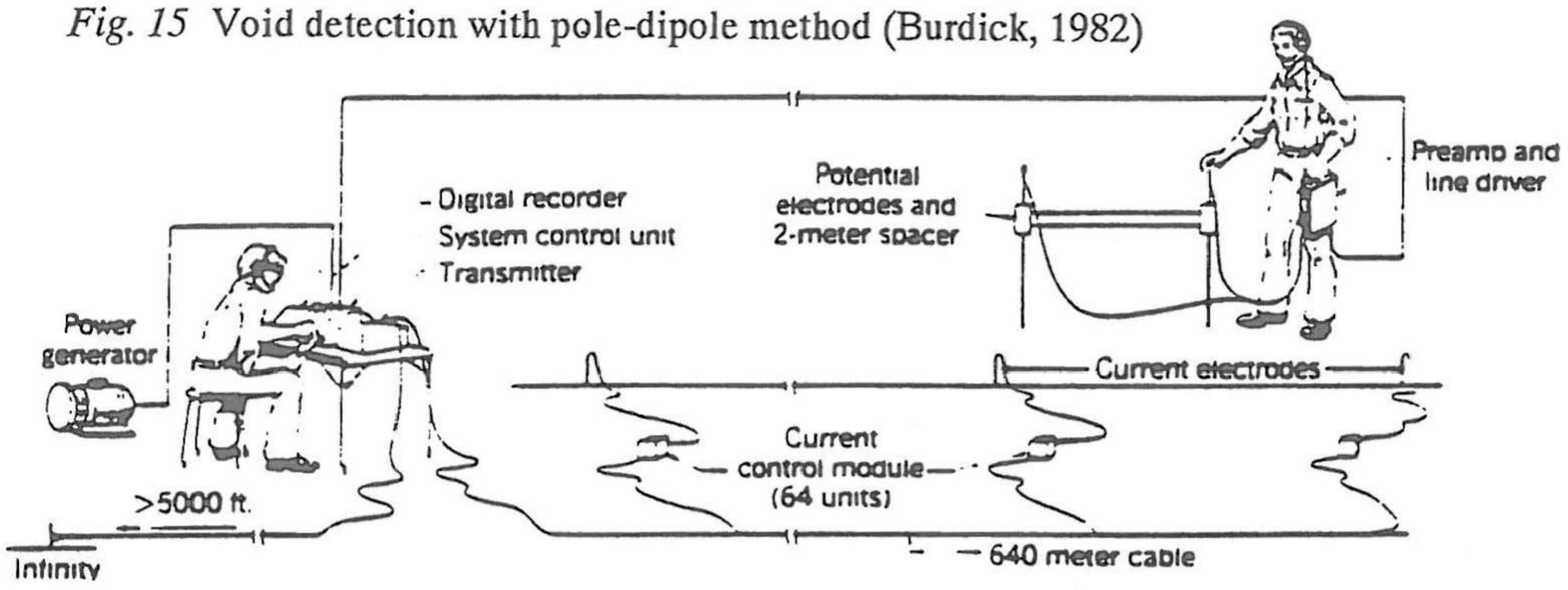

Fig. 16 Conceptual diagram of the earth resistivity data acquisition system (Peters and Burdic, 1983).

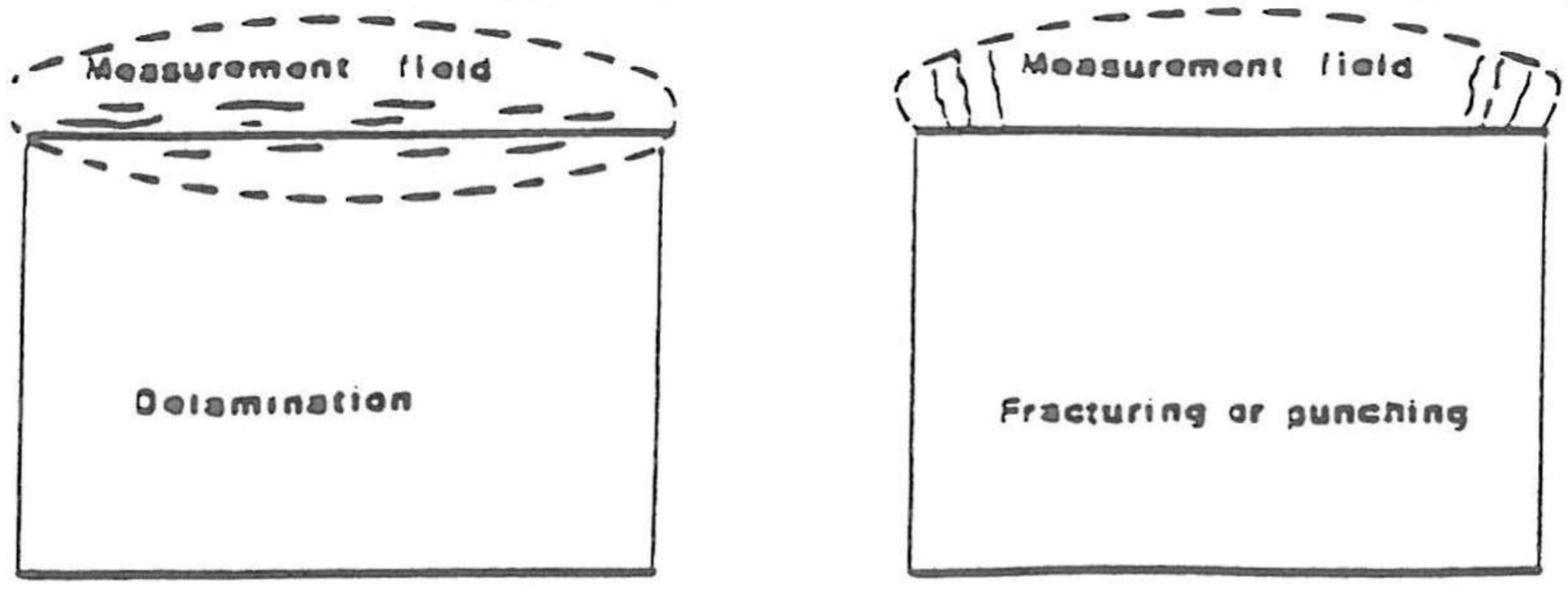

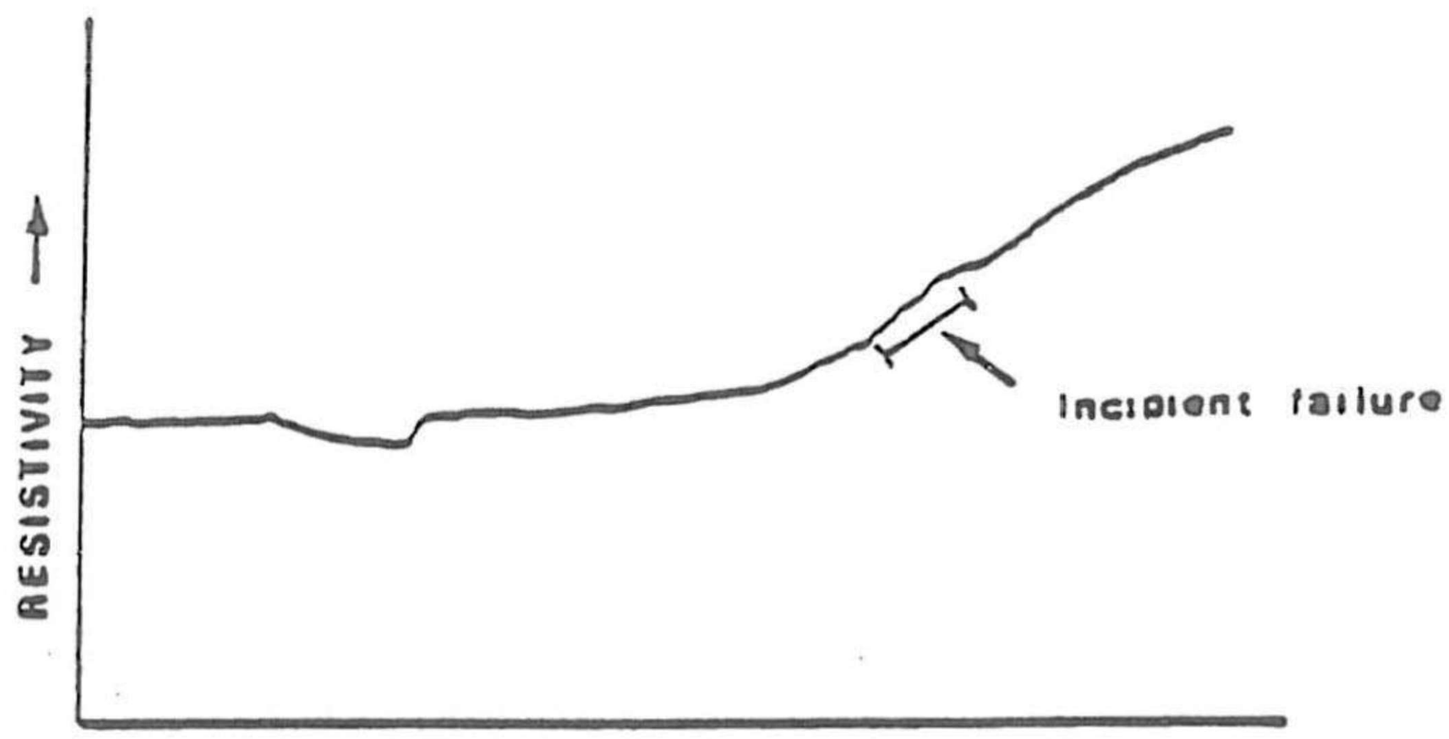

Fig. 17 Use of resistivity to predict roof falls (Burdick, 1982).

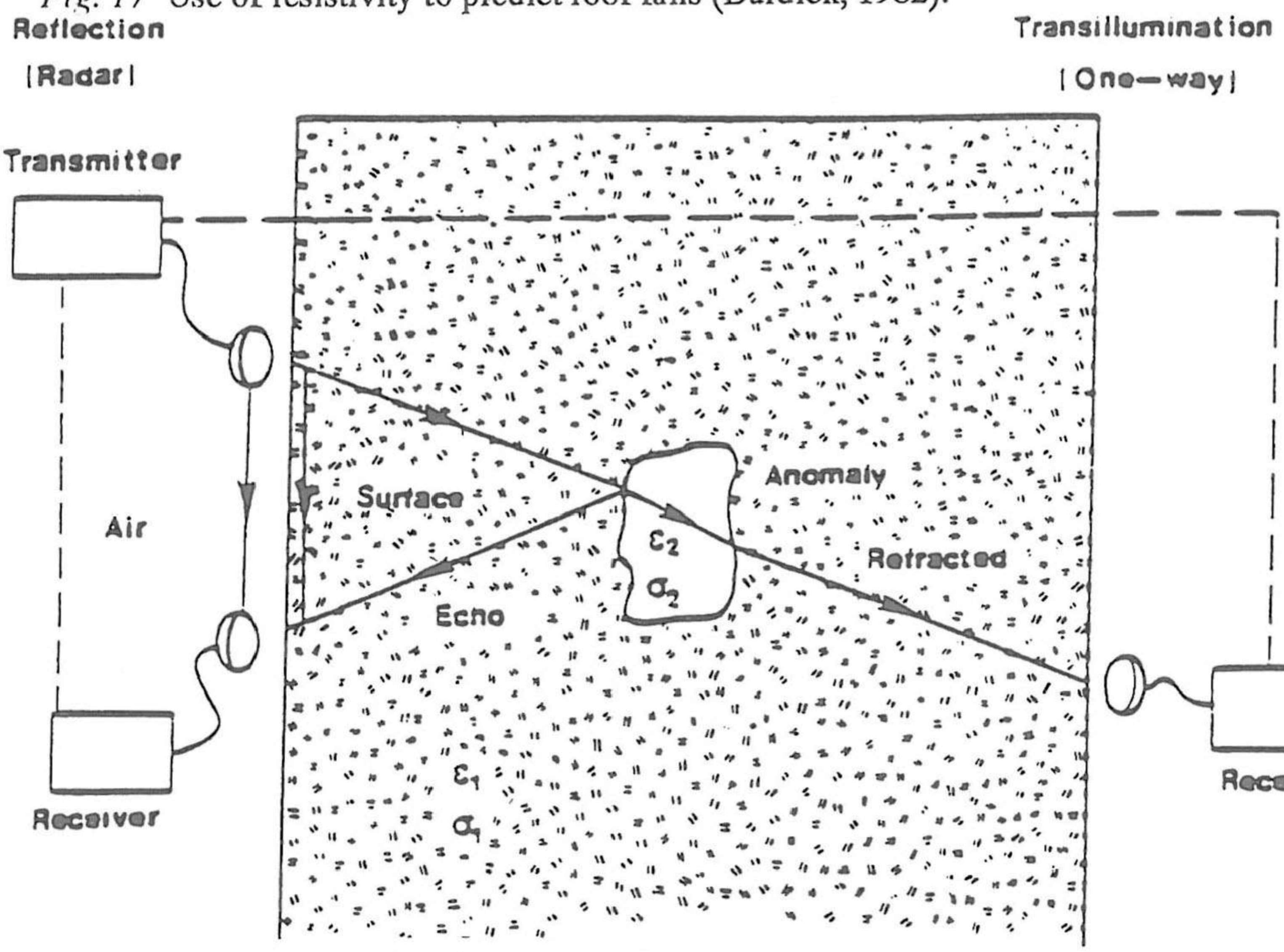

Fig. 18 Two modes of operation: reflection and transillumination. The solid black lines with the arrows indicate named travel paths of electromagnetic waves from the transmitter to receiver. ε_1 and σ_1 are the dielectric constant and conductivity of the rock media. The dielectric constant and the conductivity of the anomaly are represented by ε_2 and σ_2. The link between the transmitter and receiver is optional depending upon the technique used (Leckenby, 1982).

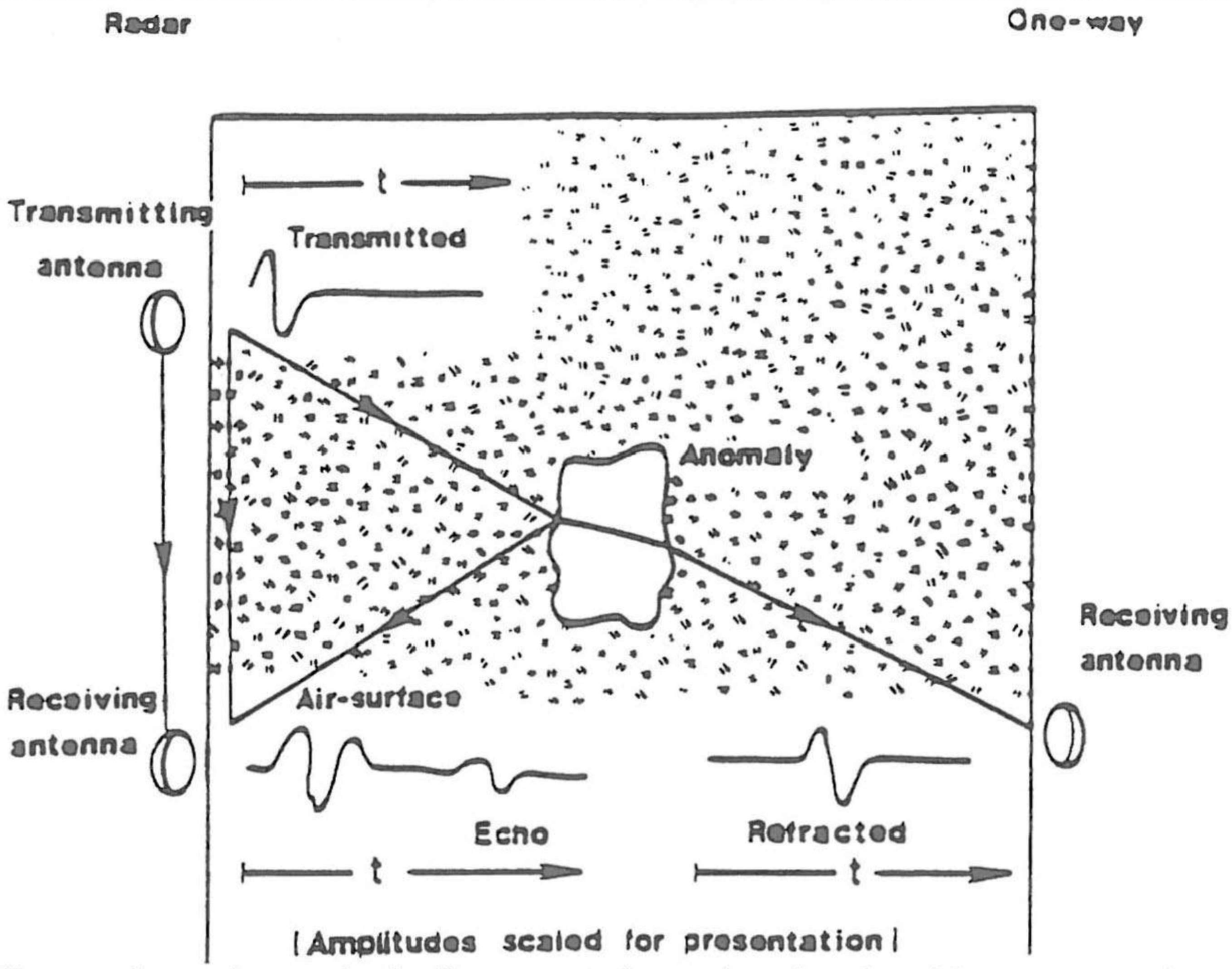

Fig. 19 Short-pulse radar methods. Representative pulse signals with respect to time, t, of the transmitted and received signals are shown for different travel paths indicated by the arrows for both radar and one-way modes (Leckenby, 1982).

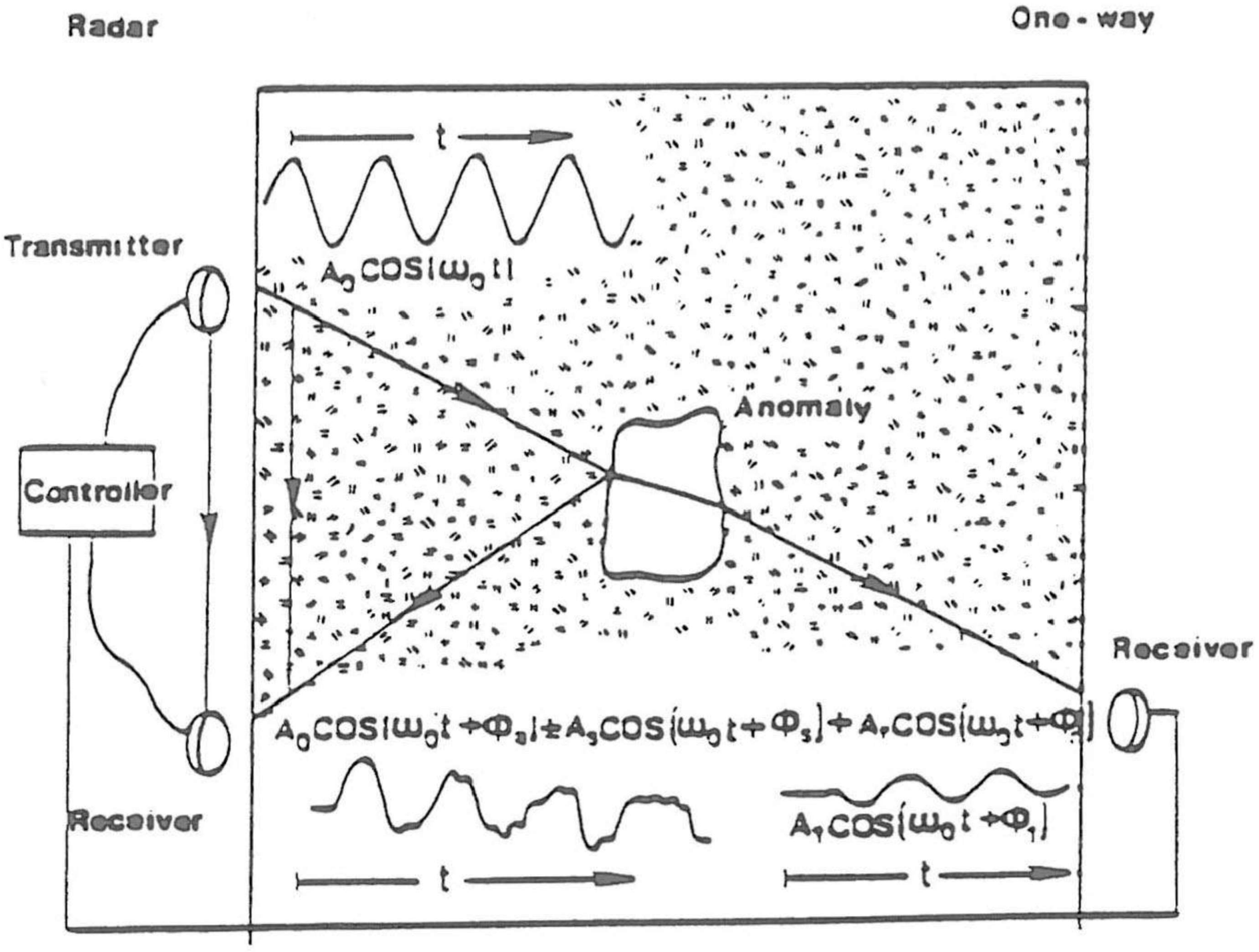

Fig. 20 Continous wave methods. Representative continous wave signals with respect to time, t, for the radar and one-way mode. A_0, A_s, A_r, and A_3 are amplitudes of the continuous waves with an angular frequency of a_0 for the transmitted surface, reflected and refracted waves, respectively. φ_s, φ_r, and φ_3 are phase constants of the surface, reflected, and refracted waves (Leckenby, 1982).

SURFACE SUBSIDENCE PREDICTION AND PREVENTION METHODS

SURFACE SUBSIDENCE PREDICTION METHODS

1.1 INTRODUCTION

Numerous methods have been developed for predicting the final subsidence and final displacement profiles (Voight and Pariseau, 1970; Brauner, 1973a; Kratzsch, 1983). But for discussion purposes, they can be classified under six categories: theoretical, profile function, influence function, graphical, physical, and numerical modeling.

The theoretical method uses theories of continuum mechanics to explain the mechanisms that lead to surface subsidence. Many models have been developed using various kinds of material behavior. These include elastic (Salamon, 1963; Berry, 1964), plastic (Pariseau, 1968), viscoelastic (Iman, 1965), and elastoplastic (Dahl, 1969).

The profile function method is essentially a method of curve fitting against the measured subsidence profiles in a particular mine or region. There are more than 20 profile functions developed empirically for nearly all major coalfields in the world. These include, to name just a few representative ones: Hungary (Martos, 1958) Japan (Hiramatsu and Oka, 1968), Russia (Avershin, 1947) United Kingdom (Wardell, 1965), and USA (Peng and Chen, 1981; Karmis et al., 1984). The NCB's graphical method in the Subsidence Engineers' Handbook (1975) also falls under this category.

The influence function method was first proposed by Bals (1931/1932). It was further developed in various periods and stages by Knothe (1957), Liu and Liao (1965), Brauner (1973a) and Marr (1975). This method is now widely accepted in various parts of the world.

The physical models include sand (Litwiniszyn, 1959; Pariseau and Dahl, 1968) and gelatin (King and Whenon, 1958; Khair et al., 1986). They are used to study the parameters that control subsidence behavior.

The most popular numerical metnod is the finite element technique. It can simulate

nearly every conceivable material behavior, heterogeneity, bedding planes, anisotropy, and various boundary conditions. This versatility is absolutely necessary considering the dynamic nature of geologic and mining conditions.

1.2 Profile function method

Among the profile functions, the negative exponential function (Peng and Chen, 1981) and hyperbolic tangent function (Hood et al., 1981; Karmis et al., 1984; Peng and Cheng, 1981) have been found applicable to the US coalfields. Both functions will be discussed in this section.

1.2.1 Negative Exponential Function

Peng and Chen (1981) developed the following negative exponential function for subsidence profiles of the major cross-sections of the subsidence basin:

$$S(x) = S_o e^{-cz^d} \tag{1}$$

where S_o is the maximum subsidence, c and d are constants, z= x/R and x is the horizontal distance from the origin, which is located at the center of the subsidence profile. R is the half width of the subsidence basin. From Eq. 1 the following equations are derived:

$$SubsidenceProfile\ S(x) = S_{oA} \tag{2}$$

$$SlopeProfile\ i(x) = \frac{S_o}{R} A' \tag{3}$$

$$CurvatureProfile\ K(x) = \frac{S_o}{R^2} A'' \tag{4}$$

$$DisplacementProfile\ U(x) = CU_o A' \tag{5}$$

$$StrainProfile\varepsilon\ (x) = \frac{CU_o}{R} A'' \tag{6}$$

where,

$$A = e^{-cz^d} \tag{7}$$

$$A' = -cdz^{d-1}A \tag{8}$$

$$A'' = cd[cdz^{2d-2} - (d-1)z^{d-2}]A \tag{9}$$

$$C = \frac{1}{A_{\max}} \tag{10}$$

$$U_o = maximum\ displacement \tag{11}$$

$$A_{\max} = maximum\ values\ of\ A' \tag{12}$$

When it comes to predicting the surface deformations on the major cross sections of the subsidence basin using Eqs. 2-6, the following critical factors must be known: maximum subsidence, S_o; maximum possible subsidence, S_{max}; maximum displacement, U_o; and constants c and d.

1.2.2 Hyperbolic Tangent Function

The general form of the hyperbolic tangent function for the subsidence profile is

$$S(x) = \frac{1}{2} S_o \left(1 - \tanh \frac{cx}{B}\right) \tag{13}$$

where S_o is maximum subsidence at the center of the subsidence profile, x is the distance from the inflection point, h is the mining depth, and c = 8.3 is a constant (Peng and Chen, 1981).

Karmis et al.(1984) however recommended a different form of hyperbolic tangent function for subsidence profiles of the Appalachia:

$$S(x) = \frac{1}{2} S_o [1 - tah \frac{cx}{B}] \tag{14}$$

where c = 1.4 for subcritical panels and 1.8 for critical and supercritical panels, and B is the distance from the inflection point to the center of the profile. The maximum subsidence S_o is influenced by the width-to-depth ratio of the opening and the lithologic characteristics of the overburden (Fig. 1). Therefore, while applying the method, the width/depth ratio of the panel and the percent of hardrock in the overburden are used to determine the maximum subsidence from Fig. 4.4. The maximum subsidence S_o obtained is then substituted in Eq. 14 for subsidence profile prediction.

Hood et al. (1981) studied subsidence profiles in the Old Ben Mine 24 in the Illinois Basin and recommended the following hyperbolic tangent function for the subsidence profiles,

$$S(x) = \frac{1}{2} S_o \left[1 - \tanh \frac{b(x-1)}{h}\right] \tag{15}$$

where b is a constant controlling the slope at the inflection point, and it varies from 7.7 to 13.3, x = horizontal distance from monument 1, and I = horizontal distance from monument I to inflection point.

1.3 Influence function method

The influence function method is applicable to the prediction of surface subsidence due to underground openings including the irregularly-shaped ones. Thus it differs from the profile function method, which can only be applied to regular openings such as rectangular or square openings.

The underlying concept for the influence function method is that the subsidence at a surface point is the sum of all surface subsidence due to the extraction of an infinite number of elements within a critical radius in the seam horizon. Accordingly, the maximum possible subsidence at the center of a critical opening is due to the mining of all elements within a radius $r = h \tan\delta_o$, where h is mining depth and δ_o is the angle of draw when the opening is within the critical width. The element just beneath the surface point of interest, has the maximum influence on the surface point. Its influence decreases as the element moves toward it and diminishes to zero for the elements located at a distance r from the projection of the surface point. In the following sections, several widely used influence function methods will be illustrated. These include the probability function method (Knothe, 1957), the Zone Area Method (Bals, 1931/32; Karmis, 1981; Peng, 1981), and the USBM Method (Adamek and Jeran, 1985).

1.3.1 Probabililty Function Method

The probability function method is one of the influence function methods. In this method, the subsidence influence on the point on the surface, a, due to the extraction of a unit element within 2r area (Fig. 2) under that point, a, follows the normal distribution function (Knothe, 1957), i.e.:

$$f(x) = \frac{1}{r} e^{-\pi(\frac{x}{\gamma})^2} \tag{16}$$

where x is the distance from the origin O. O is the vertical projection of the point, a on the seam level and r is the radius of major influence, or

$$r = \frac{h}{\tan\beta} \tag{17}$$

where h is seam depth and ß is the angle of major influence)Fig. 2).

The subsidence at surface point A due to the extraction of a unit element Δx (Fig. 2) is,

$$S_a = f(x)\Delta x \tag{18}$$

When the extraction extends from $-x_1$, to $-x_2$ (Fig. 3) for a mining height m, the surface subsidence at point A is,

$$S_A = \frac{ma}{r} \int_{-x_1}^{-x_2} e^{-\pi(\frac{x}{\gamma})^2} dx \tag{19}$$

where a is the subsidence factor and $ma = S_{max}$ is the maximum possible subsidence.

1.3.2 Zone Area or Grid Integration Method

Subsidence at a surface point P due to the extraction of an element dA within the area A (Fig. 4) is,

$$S = S_{max} \iint_A f(r)\, dA \tag{20}$$

where f(r) is the influence function and A is the extracted area.

For the horizontal seam, the influence area of a surface point is a circle, also called, the influence circle. In polar coordinates and in dimensionless form,

$$K = S/S_{max} = \iint_A f(r)\, dA \tag{21}$$

In Eq. 20 if the influence function f(r) and the limits of integration are known, the subsidence influence of a fixed area of extraction on a given surface point can be obtained. If the seam within the influence circle is totally extracted, then K= 1, i.e., subsidence at that point has reached the maximum possible value under that condition. For convenience of computation and application, the influence circle is divided into concentric circles such that the extraction of each concentric circle produces a fixed percentage of total subsidence at the point on the surface.

The zone area or the grid integration method is the true influence function method. It is applicable to subsidence prediction at any point in a subsidence basin caused by underground mining of random shape.

1.3.3 USBM Method

In testing the applicability of Bals' Method (1931/1932) for the prediction of surface subsidence for 11 longwall panels in the Northern Appalachian Coalfield, Adamek and Jeran (1985) found that Bals- Method predicts much flatter profiles than the measured ones and that corrective measures are necessary for more precise prediction.

The influence function used by Bals (1932/1933) is,

$$K = \frac{i}{h^2} \cos^2 \delta \tag{22}$$

where h is mining depth, i is unit extraction and is zone angle of the influence circle (Fig. 5).

Based on Bals' Method, Adamek and Jeran (1985) obtained some predicted subsidence profiles for the Northern Appalachian Coaifield when $\delta = 15^\circ$ and $\delta = 25^\circ$ were used (Fig. 6). There are considerable differences between the predicted and the measured profiles, and furthermore, the difference can not be made up by merely changing the angle of draw. Adamek and Jeran (1985) attributed the difference to the existence of strong but lightly loaded sandstone and limestone overlying the Pittsburgh seam. In order to make it applicable to the Appalachian Coalfield they modified the expression for subsidence prediction to,where m is mining height at ith point, e_i is efficiency coefficient, and a_{vi} is he variable subsidence

$$S_i = m e_i\, a_{vi} \tag{23}$$

coefficient at the ith point.

Adamek and Jeran (1985) stated that in the revised method, e_i reflects the special

features of the Bals' Method, while a_{vi} accounts for the influence of profile function method.

1.4 Graphical method

The best known graphical method is the UK NCB's (now British Coal or BP) Subsidence Engineer's Handbook (1975). The method is illustrated as follows:

1. When the length of the gob, $L_1 \geq 1.4\ h$, the subsidence factor, $a_o = S_{max}/m$, can be found in Fig. 7 for corresponding width, L_2, and depth, h, of the panel. Then the maximum possible subsidence can be determined by $S_{max} = a_o m$.
2. When $L_1 < 1.4\ h$, the maximum subsidence, S_o, is less than S_{max}. Thus a correction factor must be applied to S_{max} obtained in step 1. The correction factor, S_o/S_{max}, for corresponding L_1/h and depth can be located by using Fig. 8.
3. The subsidence profile on a major cross-section can be predicted by the nomograph shown in Fig. 9. Obviously the subsidence profile is closely related to L_1/h. Notice that each curve represents the predicted subsidence in terms of maximum possible subsidence, S_{max} (or S_o), at the panel center.

The NCB method is the result of averaging data from about 165 longwall panels and represents an overburden consisting predominantly of shale and siltstone. Under similar conditions, such as those in the Illinois coal basin, the NCB method can accurately predict the maximum subsidence, but not the subsidence profile (Munson and Eichfield, 1980). In studies where the overburden differs significantly from the NCB cases, the correlation between the actual subsidence and the predicted value by the NCB method does not agree as closely as in the Illinois case (Sutherland and Schuler, 1981). Studies also show that the NCB method always predicts much larger maximum subsidence at panel center as compared to the measured data in the Appalachian Coalfield.

1.5 Finite element method

The finite element method is a very versatile tool for solving geomechanical problems, because it can incorporate parameters such as local variations in geological conditions which are almost the rule in underground coal mines. It can also handle changing boundary conditions, and most important of all, any material behavioral models can be modeled. The theory of the finite eletnent method is well-documented in the literature (Zienkiewicz, 1977). Some special applications of the method applied to subsidence prediction are covered in this section.

The best example of using the 3-dimensional finite element method for predicting surface subsidence due to underground coal mining is the elastic-elastoplastic model

performed by Choi and Dahl (1981). The model is linearly elastic until the Coulomb yield criterion is satisfied. The incremental constitutive equation is,

$$d(\sigma) = E\, d(\varepsilon) \tag{24}$$

where d(σ) and d(ε) are incremental stress and strain, respectively. The Young's modulus, E, is the proportionality constant of stress and strain. E is linear below the yield point, whereas for applied stress above the yield point, E is stress-dependent as specified by the yield criterion. E and T_o (tensile strength) for various parts of the model are different as shown in Fig. 10. Poisson's ratio and the angle of internal friction are held constant at 0.25 and 30°, respectively.

Fig. 11 shows the subsidence contours as predicted by the model. Notice that only a quarter of the rectangular panel is shown. As compared to the actual subsidence measurements the model predicts reasonably well inside the panel edges. Beyond the panel edges above the solid coal the model predicts much wider influence zone. The major horizontal strain parallel to the faceline is compressive at the panel center with a maximum of 3.2 mil/in., whereas around the panel edge tensile strain prevails, the maximum of which is 1.2 mil/in. It must be emphasized that the model assumes homogeneous material composition, and disregarded the stratigraphic sequences in the overburden, and that the material properties used in Fig. 10 were obtained from the results of the laboratory tests by a reduction factor of 10 or 20.

In 2-D modeling the Drucker-Prager yield criterion has also been applied to predict the subsidence profiles for 10 longwall panels by Siriwardane (1985) and his staff (Siriwardane and Amanat, 1984a and 1984b). i.e.,

$$\sqrt{J_{2d}} - \alpha J_1 - k = 0 \tag{25}$$

where δ_1, δ_2 and δ_3 are the maximum, intermediate and minimum principal stresses,

$$J_{2d} = 1/6\, [(\delta_1 - \delta_2)^2 + (\delta_2 + \delta_3)^2 + (\delta_3 - \delta_1)^2]$$

$$J_1 = \delta_1 + \delta_2 + \delta_3$$

$$\alpha = \sin\varphi[3(3 - \sin^2\varphi)]^{-1/2}$$

$$k = 3C\cos\varphi[3(3 - \sin^2\varphi)]^{-1/2}$$

respectively. φ is the internal angle of fnclion and C is the cohesive strength.

Siriwardane and Amanat stated that the validity of the finite element model for subsidence prediction can be evaluated in terms of maximum subsidence and shape (i.e., in terms of S/S_{max}) of the subsidence profile. Strata in the overburden were simulated in the model. The emphasis on their work was on predicting the shape of the normalized subsidence profile. This study indicated that when the cohesive strength is reduced to 1/100, the nonlinear model predicts much closer to the field subsidence profile than the linear one. However, in order to match the predicted maximum subsidence with the field value, the elastic modulus of the region under yield state needs to be reduced by a factor. This reduction factor was 1/67, for the above mine, but was different for each mine

analyzed. Regardless of the reduction factor, the shape of the subsidence profile did not change significantly (Fig. 12). Siriwardarie and Amanat (1984b) also recommended that in order to eliminate the boundary effects, the model size must be on both sides at least five times the half-width of the panel away from the centerline of the panel, and five times the thickness of thie coal seam below the seam floor, and also that the initial stress method (Zienkiewicz, 1977) must be used for accurate modeling of the initial stress in the model, because in the stratified model, due to difference in elastic properties, the initial horizontai stress in various strata is not uniforrn as normally assumed. Their parametric analyses also showed that the shape of the subsidence profile is influenced by cohesive strength C when it is larger than 1/100 and that the angle of internal friction , and the Young's modulus E, do not appear to have significant influence on the shape of the profile, although they do exert significant influence on the maximum subsidence at the panel center.

SURFACE SUBSIDENCE PREVENTION METHODS

PREVENTION OF DAMAGE TO SURFACE FACILITIES

Preventive ways to minimize surface structural damage can be categorized as either surface structural protection or underground controlled mining. At the surface, new structures may be designed to resist or accommodate the effects of subsidence; existing structures can be modified to minimize damage. Below the surface, mining can be accomplished by various mining techniques to minimize surface subsidence and surface strains.

2.1 Structural Protection

New structures maybe designed to minimize changes in design force (flexible design) or to reduce the total distortion (rigid design) of the structures, or both. In the flexible design approach, structural elements are flexible and deflect according to the subsidence profile. The base elements and foundation are therefore kept in intimate contact with the ground as subsidence proceeds. This can be accomplished by special foundation and structural designs. Figure 13 shows a foundation arrangement for the flexible design. A 6-in. layer of compacted sand is laid directly on top of the bedrock. A layer of building paper or polythene is then inserted to separate the sand layer from an overlying 6-in. concrete slab. The underside of the slab should be free from any projection, and its top should be near the level of the finished ground surface. The concrete slab is further reinforced at top and bottom to accommodate tensile and compressive strains. The compacted sand layer in this design minimizes the amount of strain transmitted from the ground to the concrete slab and in the meantime allows it to assume the ground shape as

it deforms. The superstructure should be as light as possible and capable of deflecting sufficiently to follow the differential vertical movement without cantilevering.

Rigidly designed structures allow cantilevering and spanning over a subsidence and involve heavy structural elements capable of sustaining high shear forces and moments. Therefore releveling jacks are usually installed at strategic points in the foundation to maintain the horizontal position of the structure. The foundation design for a rigid system is similar to that of flexible system except that it uses strongly reinforced concrete rafts or beams capable of supporting the superstructures.

The length of a building is important design criterion. A longer building may be constructed on ground that is in part subjected to the maximum strain, whereas a short, small building is more likely to be erected in an area of uniform strain. Where large buildings are required, they must be separated into small units with a gap of at least 2 in. between each pair of units. The gap should be free from any obstruction and extend into the foundation. Furthermore the long axis of a large building should be parallel to the subsidence contour lines rather than perpendicular to them, which distributes the strain uniformly on the building.

For old buildings located in a subsidence area, several preventive measures are used:

2.1.1 Temporary removal of the building.

The entire superstructure of smaller buildings can be separated from the basement foundation and moved by usual house-moving methods to an unaffected area during mining. When subsidence ceases after mining, the foundation, if damaged, is repaired and the superstructure is then reinstalled.

2.1.2 Internal bracing and leveling.

I-beams of sufficient strength are installed on the ceiling of the basement, and in directions both parallel and perpendicular to the direction of mining. Each I-beam is supported by several hydraulic jacks or equivalent supports at a suitable spacing. The settlement of the I-beam is monitored during the period of undermining. Any differential settlement on the I-beams must be corrected immediately by adjusting the hydraulic jacks. To ensure success by this method, the settlement of the I-beam must be inspected and, if needed, adjusted as often as possible, say once per day or per shift during undermining.

2.1.3 Trenching.

A trench is excavated around the building , a yard from the external wall (Fig. 14). The width of the trench need not be more than that required for digging, but it should extend to the foundation. The trench can be filled with compressible materials and covered with concrete slabs. A reduction of 50 % in structural damage has been reported with trenching (NCB, 1975), but it is more effective in coping with compressive ground strains than tensile ones.

2.1.4 Cutting of walls.

Building and brick walls of structures longer than 60 ft can be cut to reduce damage (Fig. 15). The resulting gap should be wide enough to accommodate deflection. The cut should also be extended to the foundation and incorporated into a trench if possible.

2.1.5 Taping.

Large glass windows should be taped to avoid flying glass that can result from compressive strain.

2.1.6 Banding and strapping.

If structures are extremely weak in tension, they can be reinforced by strapping or tie bolting.

When subsidence occurs, a completely flexible pipeline will deflect to assume the subsidence profile, but a rigid buried pipeline will become unsupported and be subjected to an increasing load of the overlying soil. Therefore the principle of pipe laying involves the prevention of excessive loading. This can be accomplished by constructing a well-compacted soil arch over the pipe as shown in Fig. 16. Another technique called the imperfect ditch method of construction (Baker, 1974) uses straw, hay, sawdust, or cornstalks for imperfect ditch backfill. It is effective in greatly reducing the pressure on pipelines by creating an arched support in the overlying soil and can be applied to both rigid and flexible pipelines. Pipeline joints should also be flexible and telescopic to provide sufficient deflection, straight draw, and line displacement. For the old buried pipelines without such preventive measures, the best way is to dig it out and have it exposed. Its settlement during undermining is then monitored closely and leveled when required.

Driveway pavements, parking areas, and highways should be of asphalt, macadam, or some other flexible material with a granular foundation to reduce the amount of strain transmitted from the ground to the pavement. Similarly surface water drainage systems and culverts should be articulated to reduce damage.

2.2 Underground Controlled Mining

Underground controlled mining involves techniques that do not produce surface subsidence exceeding the allowable limits and is therefore effective in reducing surface damage. Several methods frequently employed in coalfields are illustrated here.

2.2.1 Panel Layout Design

In laying out a panel, attempts should be made to avoid placing the structure on a location where the ground deformation sensitive to that structure is at its maximum. Therefore rational design of the panel is the simplest way to reduce structural deforma-

tions. Panel design involves the determination of panel dimension, panel edge location, and direction of face advance.

(a) Panel Dimensions.

Since the U.S. Longwall employs multiple-entry system where rows of chain pillars are left unmined, subsidence over those chain pillars are usually very small. Therefore, whenever possible, the panel dimension should be designed such that a major structure or structures lie over unmined chain pillars between adjacent panels or some distance beyond both ends of the panels.

At the center of the supercritical final subsidence basin, a structure will not be subjected to any final and permanent ground deformations. In order to create such a condition, the panel must be located such that the structure will be at the center of the opening or the final mined-out gob, whose minimum dimension must be

$$L = D + 2h \tan\delta_o \tag{26}$$

where L is the width or length of the final mined out gob, D is the width or length of the structure to be protected, h is mining depth, and $_o$ is the angle of draw.

(b) Panel Edge Location.

Wherever there is a permanent panel edge, there are large ground deformations induced on the surface on both sides of the permanent panel edge. Therefore it is important to determine the optimum location of the permanent panel edge with respect to surface structures.

In terms of permanent edge location, the best way is to eliminate any permanent panel edge under a structure or groups of structures. If this cannot be done, the panel should be lengthened to reduce the number of permanent panel edges, or narrower but multiple panel advancing should be employed in the same direction in a staggered manner.

(c) Direction of Face Advance.

The direction of face advance should be parallel to the long axis of the structure. But if the structure is to be located at the center of the final subsidence basin, the direction of face advance should be perpendicular to the long axis of the structure.

The direction of multiple-face advance is utilized most effectively to reduce structural deformation and thus damage. One applies the principle of overlapping and cancelling ground deformations due to multiple-face advance at the right time and at the right intensity, e.g., opposing tilts, concave vs. convex curvature, or tensile vs. compression induced simultaneously on the structure to be protected by two or more faces.

2.2.2 Partial Extraction

Surface structures can be protected by partial extraction, using the room-and-pillar, board-and-pillar, or panel-and-pillar method. For example, in Pennsylvania the extent of support for a structure is determined by providing a zone 15 ft wide from the periphery of

the structure. This area is then projected downward and outward at an angle of 15 from the vertical until it reaches the seam level. Unmined pillars in this projected area should be left at least equivalent in area to 50% of the total area to prevent excessive subsidence (Fig. 17).

In Europe, however, the panel-and-pillar system is frequently used with relatively long but narrow parallel panels separated by permanent pillars (Fig. 18). Panels and pillars are the same width, which is approximately one-fourth of the seam depth. The observed surface subsidence ranges from 3 to 20% of the seam thickness. However, subsidence increases with depth of mining due to greater deformation incurred on the pillars.

2.2.3 Harmonic Extraction

The structure to be protected is undermined with staggered faces as shown in Fig. 19. The numbers in the figure indicate the mining sequence. The structure is located on the common edge of two adjacent panels. The right-side panel is mined first and kept at a fixed distance ahead of the left-side panel, approximately equal to one-fourth of the critical width. The tensile strain traveling with the face for the right-side panel is relatively small over this edge, while the compressive strain behind the face will to some extent be compensated by the traveling tensile strain from the left-side panel. This way the strain induced at the site of the structure is kept at a minimum.

2.2.4 Rapid Mining

The maximum tensile strain, E_t, traveling with an advancing face is generally less than the final obtainable tensile strain, E_{max} (Fig. 20), and the faster the mining proceeds, the smaller the E_t. Furthermore the maximum compressive strain accompanied with the traveling face is always less than the corresponding maximum tensile strain, E_t. Therefore there exists a minimum rate of mining, characteristic of each coalfield that will induce a maximum tensile traveling strain that is smaller than the allowable one.

2.2.5 Towing

Since the amount of subsidence is proportional to the excavated seam height, it can be reduced by stowing. Table 1 indicates the subsidence factors for various methods of stowing in various coal fields. The wide range of subsidence factors for each coal field is due to the difference in material properties and stowing procedures; More compacted stowing allows smaller subsidence, and stowing procedures that permit stowing to be performed immediately after mining induce smaller subsidence than if stowing can be done long after mining.

REFERENCES

1. Peng, S. S., 1986, Coal Mine Ground Control, Second Edition, John Wiley and Sons, New York, pp. 451-460.

2. Peng, S. S., 1992, Surface Subsidence Engineering, 1st Edition, SME Inc., Littleton, Colorado.

Table 1 Subsidence factor and ratio of Maximum Horizontal Displacement to Maximum Possible Subsidence

Coal Field and Method of Packing	Subsidence Factor	Ratio
British coal fields (8)		
Solid stowing	0.45	0.16
Caving or strip-packing	0.90	0.16
Ruhr coal field, Germany		
Pneumatic stowing	0.45	0.35 – 0.45
Other solid stowing	0.50	0.35 – 0.45
Caving	0.90	0.35 – 0.45
North and Pas de Calais coal field, France		
Hydraulic stowing	0.25 – 0.35	0.40
Pneumatic stowing	0.45 – 0.55	0.40
Caving	0.85 – 0.90	0.40
Upper Silesia, Poland		
Hydraulic stowing	0.12	—
Caving	0.70	—
U. S. S. R.		
Donbass district	0.80	0.30
Lvov-Volyn district	0.80 – 0.90	0.34
Kizelov district	0.40 – 0.80	0.30
Donets, Kuznetsk, and Karaganda districts	0.75 – 0.85	0.30
SubMoscow and Cheliabinski districts	0.85 – 0.90	0.35
Pechora	0.65 – 0.90	0.30 – 0.50
U. S. A.		
Eastern (room and pillar) (9)	0.10 – 0.60	—
Central (longwall) (10)	0.50 – 0.60	—
Central (room and pillar) (10)	0.10 – 0.40	—
Western (5, 6)	0.33 – 0.65	—

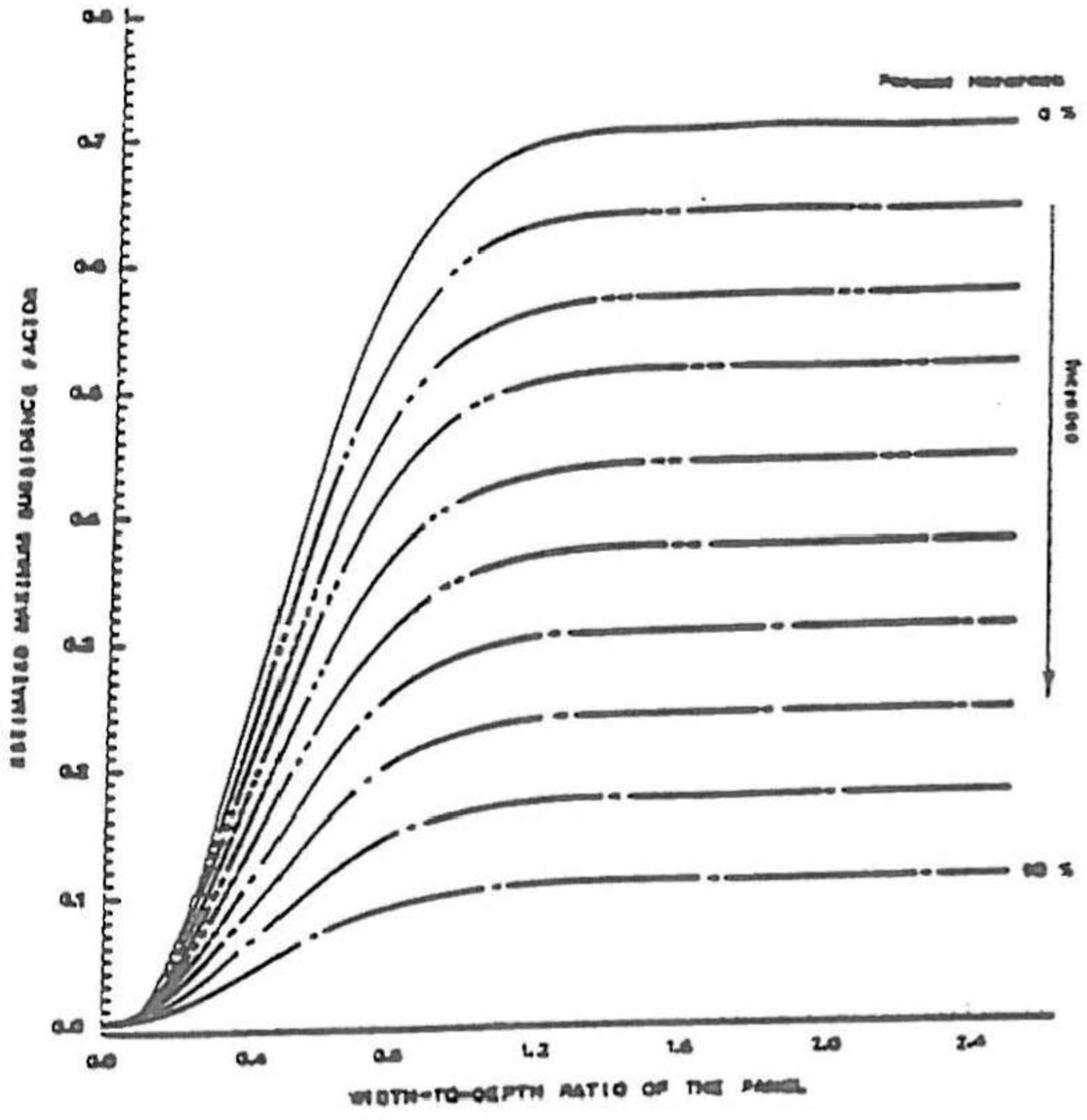

Fig. 1 Effect of lithology and width/depth ratio on the maximum subsidence. (Karmis et al. 1984).

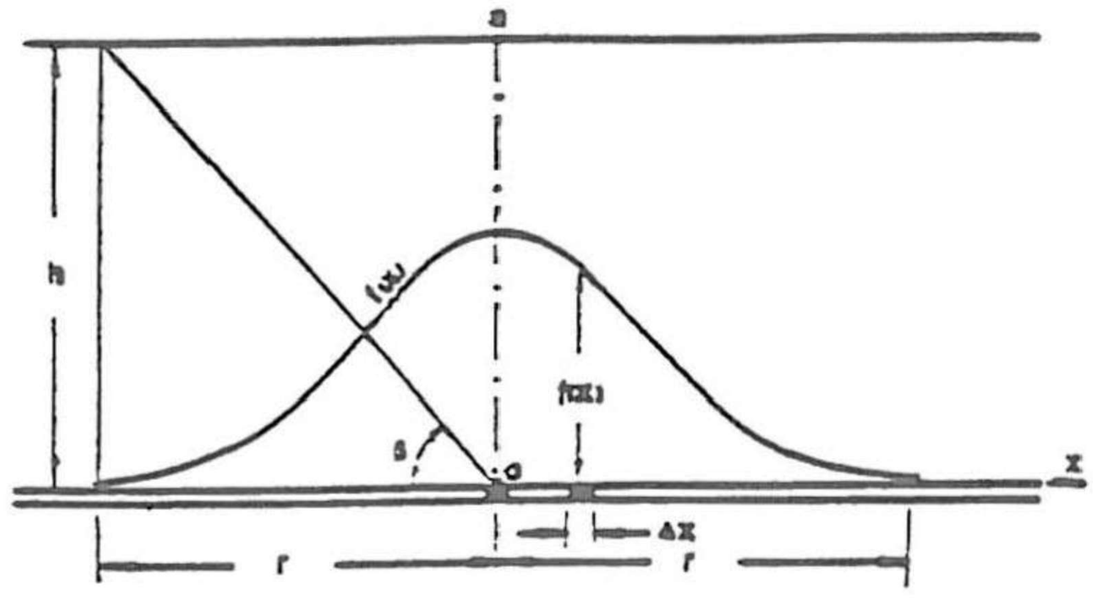

Fig. 2 Scheme of the influence on the subsidence at surface point.

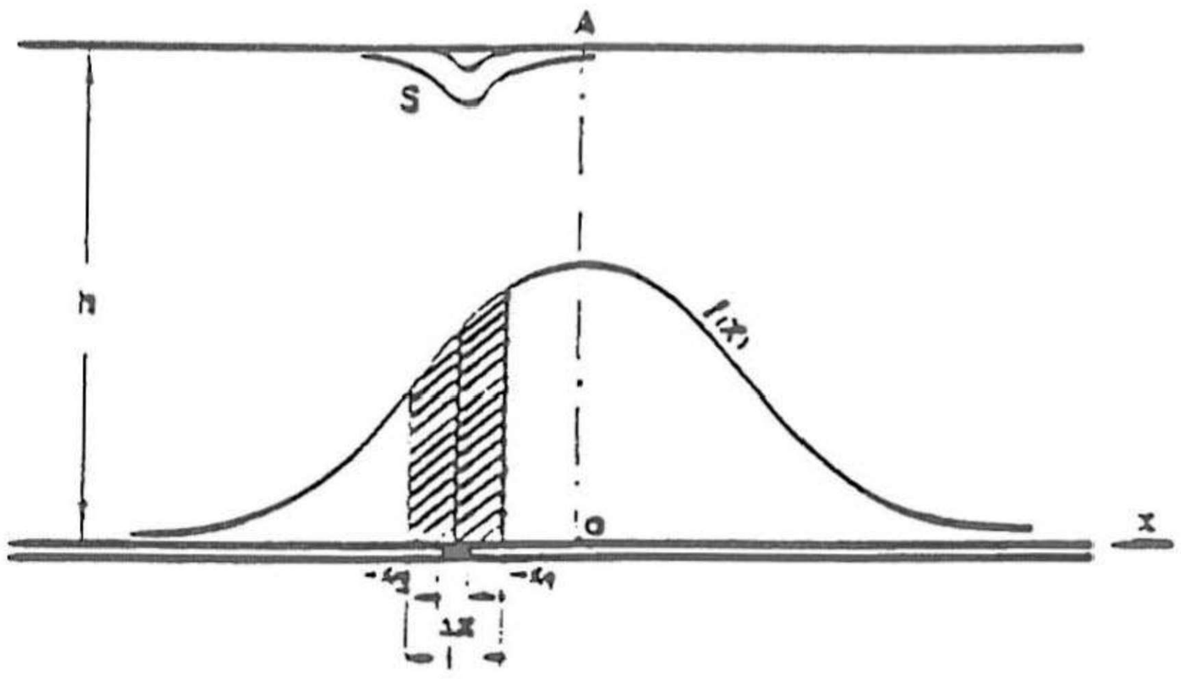

Fig. 3 Calculation scheme of the surface subsidence at point A due to extraction from $-X_1$ to $-X_2$.

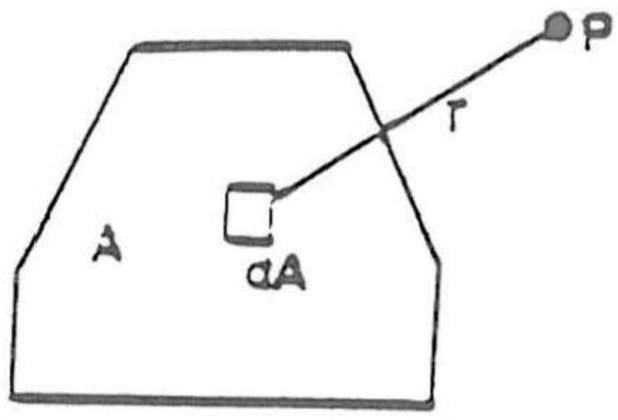

Fig. 4 Principle of zone area or grid integration method.

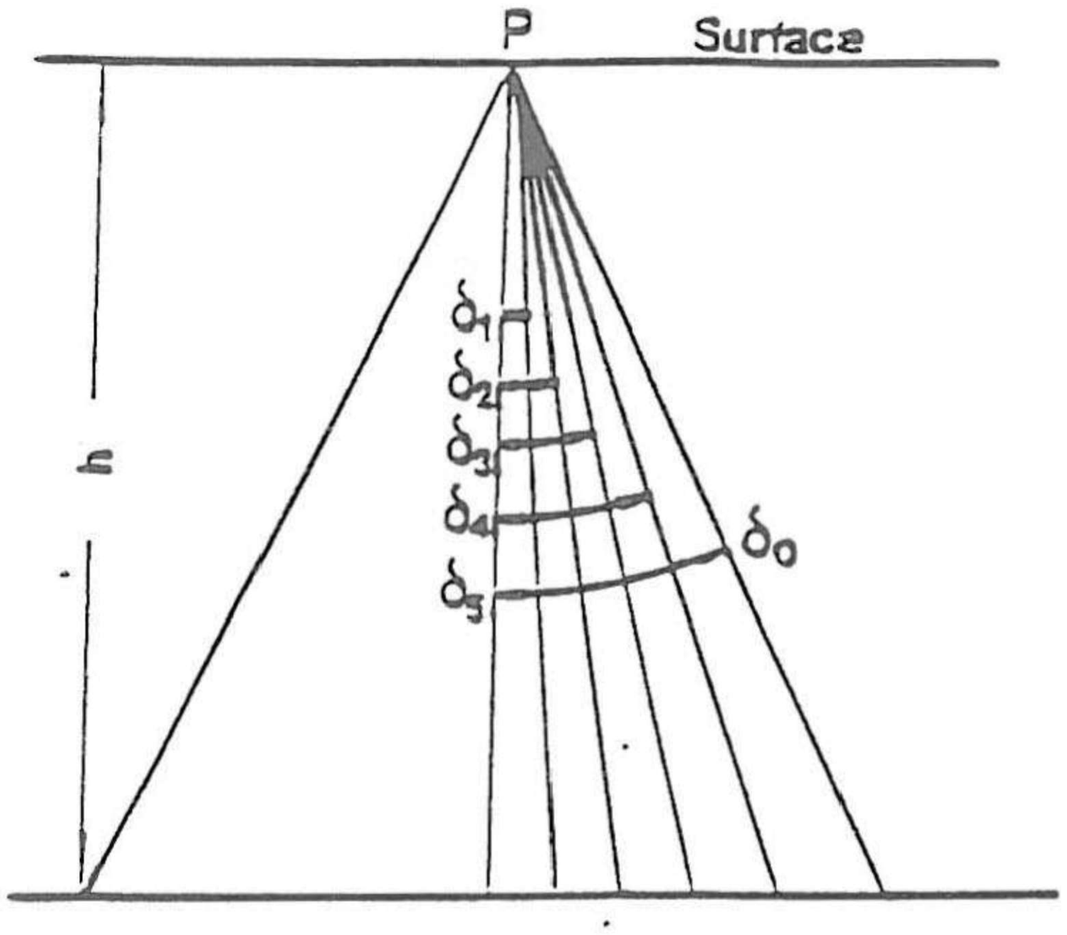

Fig. 5 Bals' division angles.

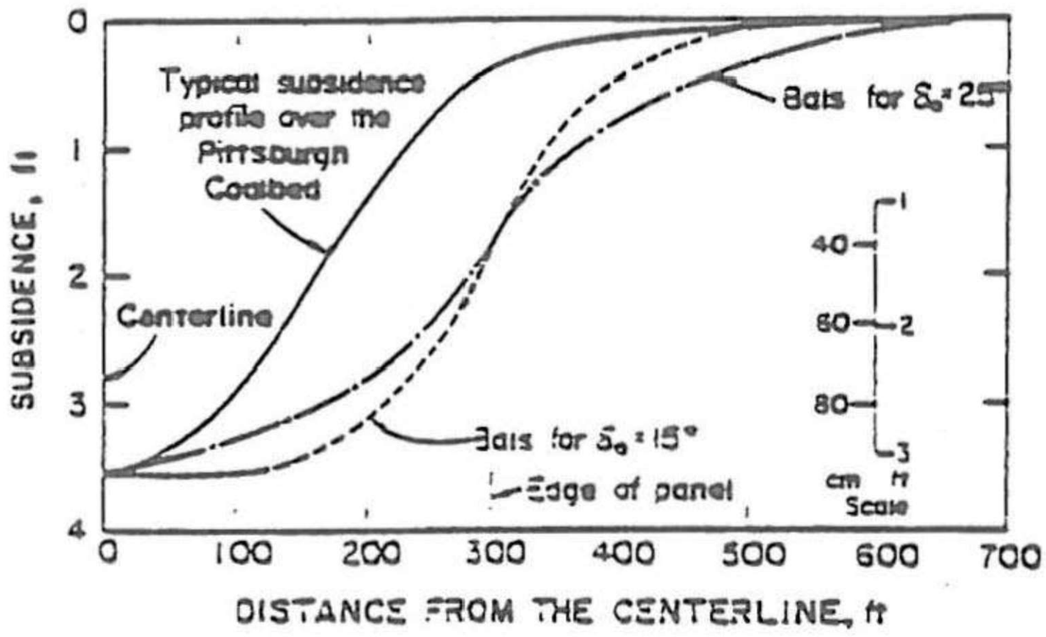

Fig. 6 Comparison of subsidence profiles between measured and that predicted by Bals' method (Adamek and Jeran, 1985).

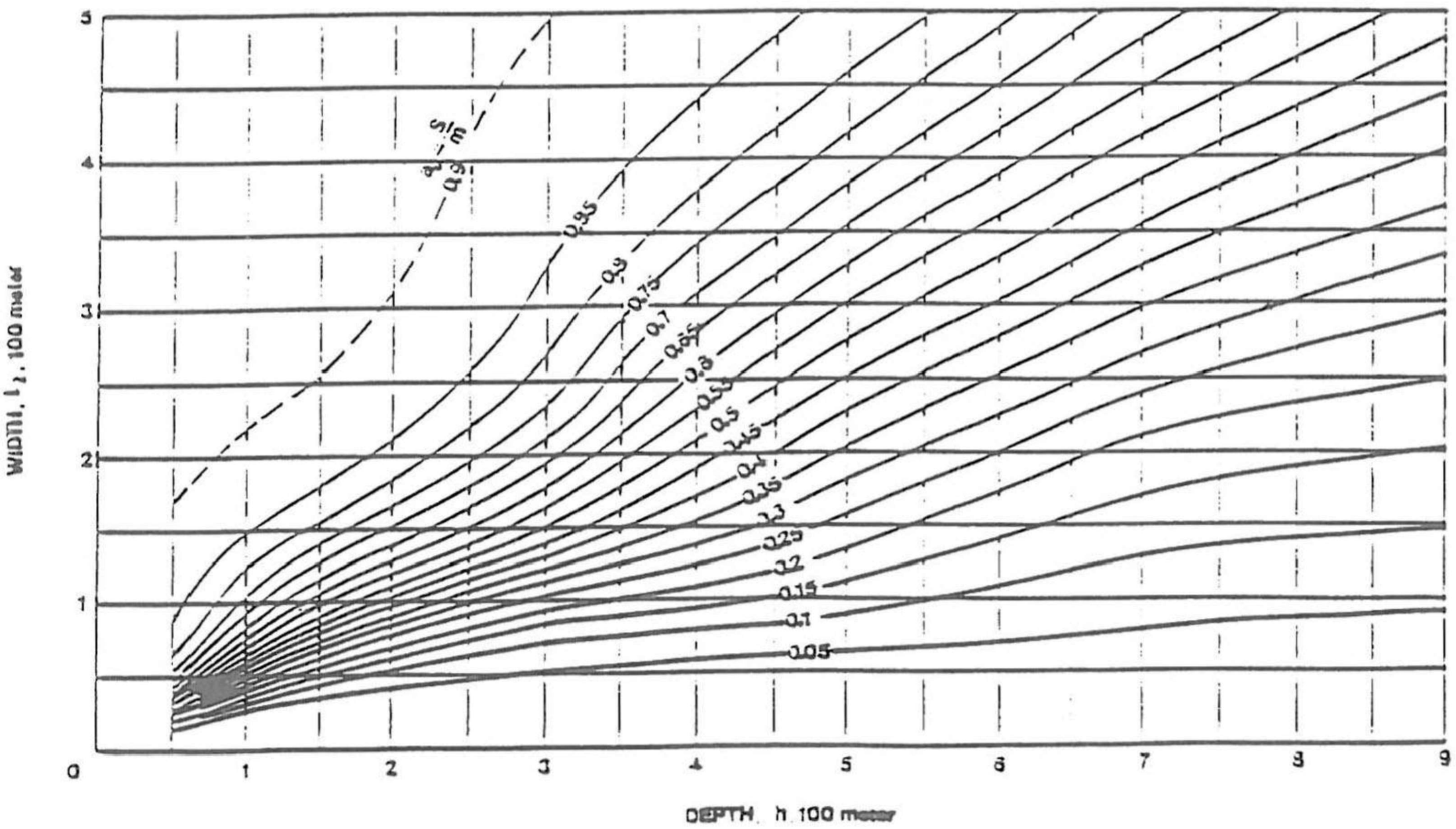

Fig. 7 Nomograph for determining the subsidence factor (NCB, 1975).

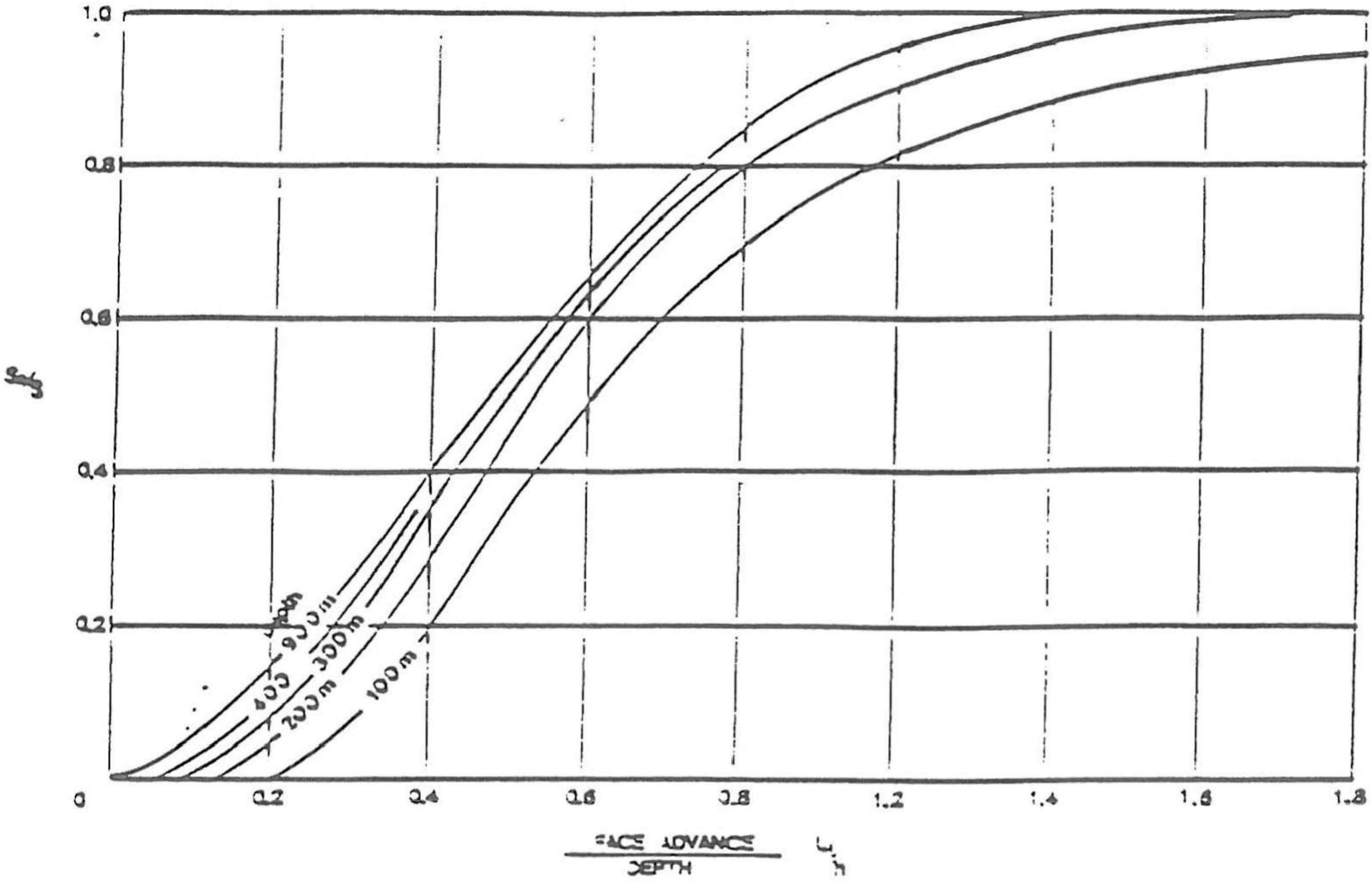

Fig. 8 Nomograph for determining the correction factor for semicritical openings (NCB, 1975).

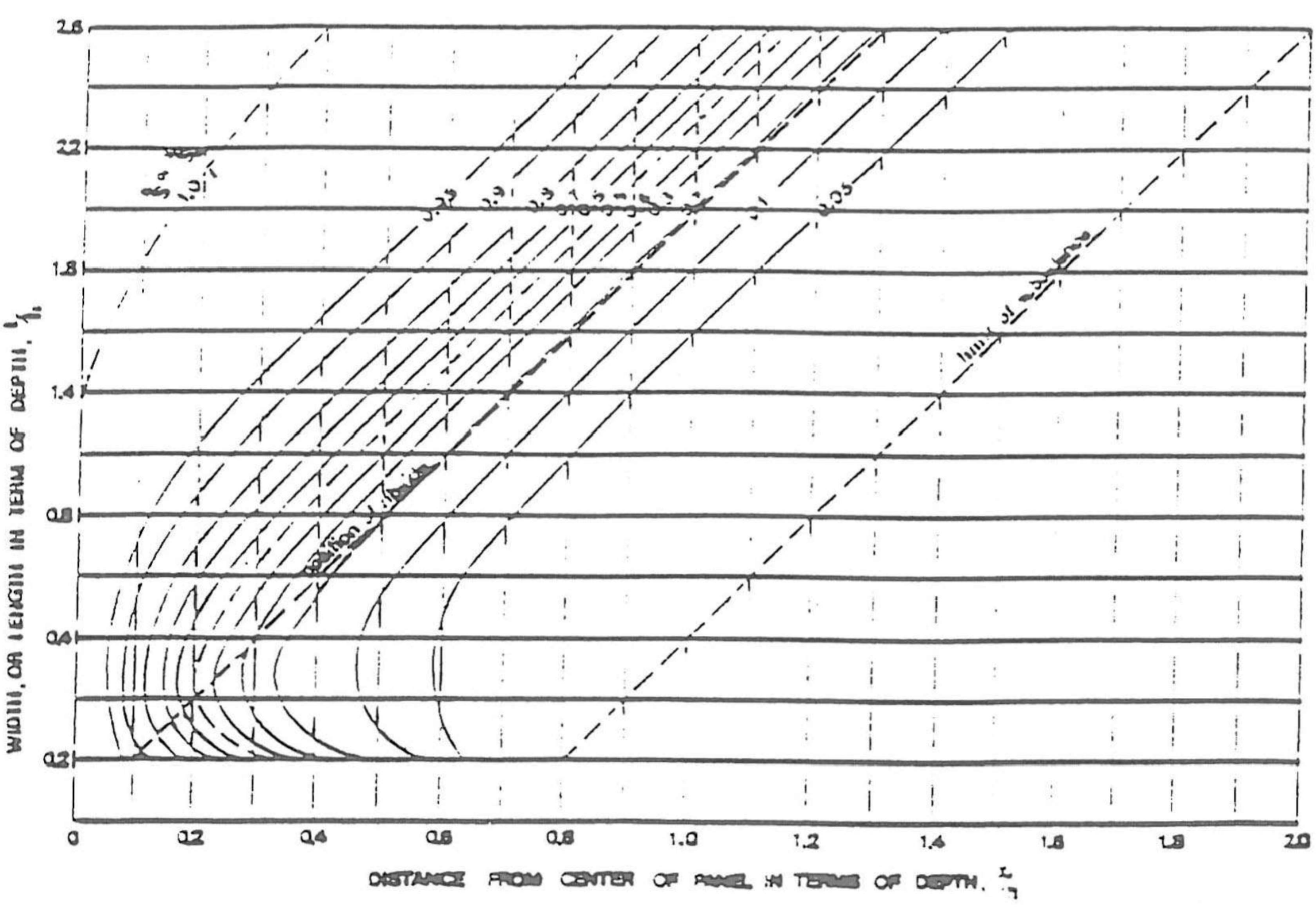

Fig. 9 Nomograph for predicting the subsidence profile (NCB, 1975).

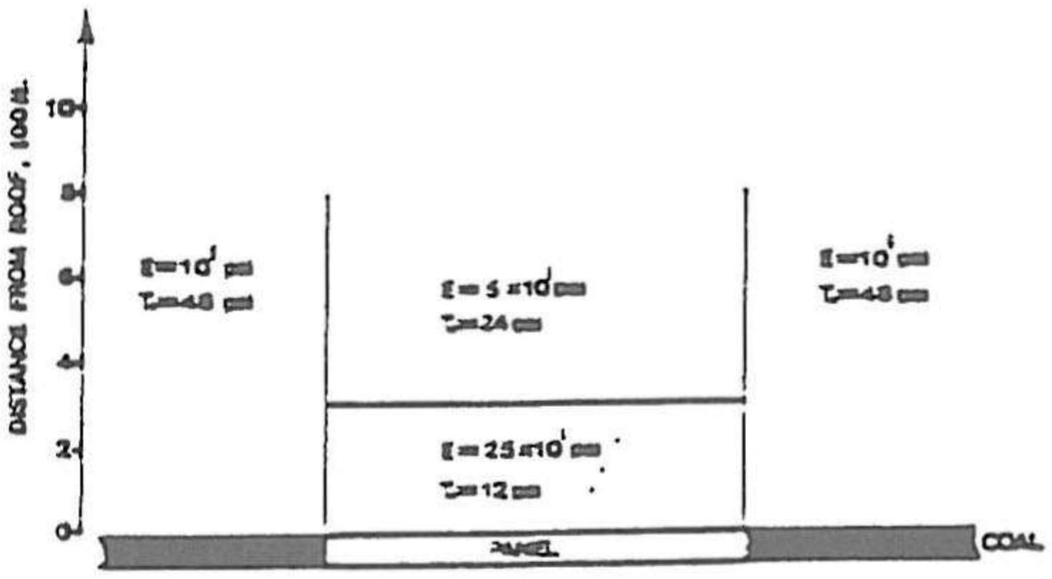

Fig. 10 Material properties used in 3-D finite element model by Choi and Dahl (1981).

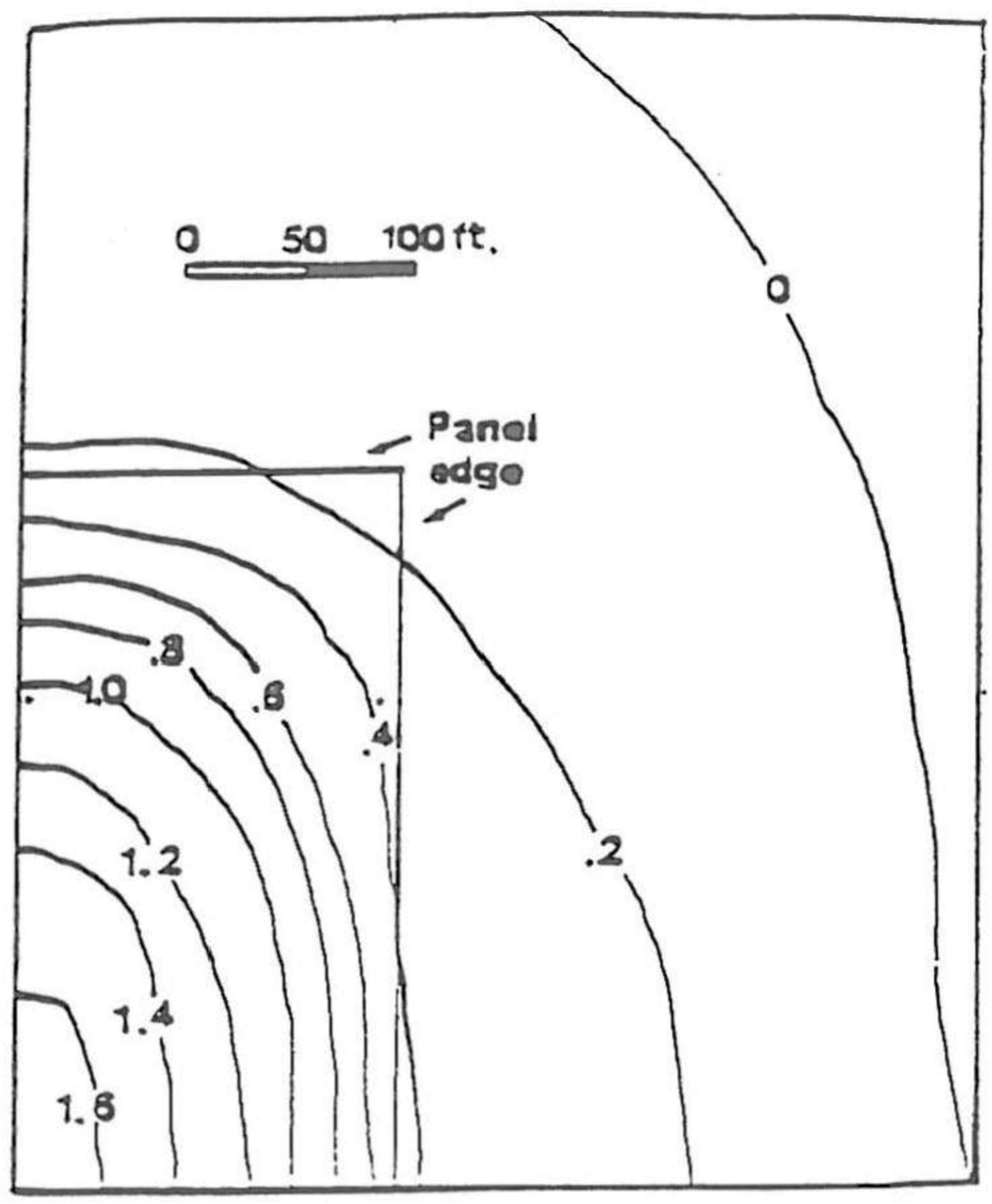

Fig. 11 Predicted subsidence contours, in ft. by Choi and Dahl (1981).

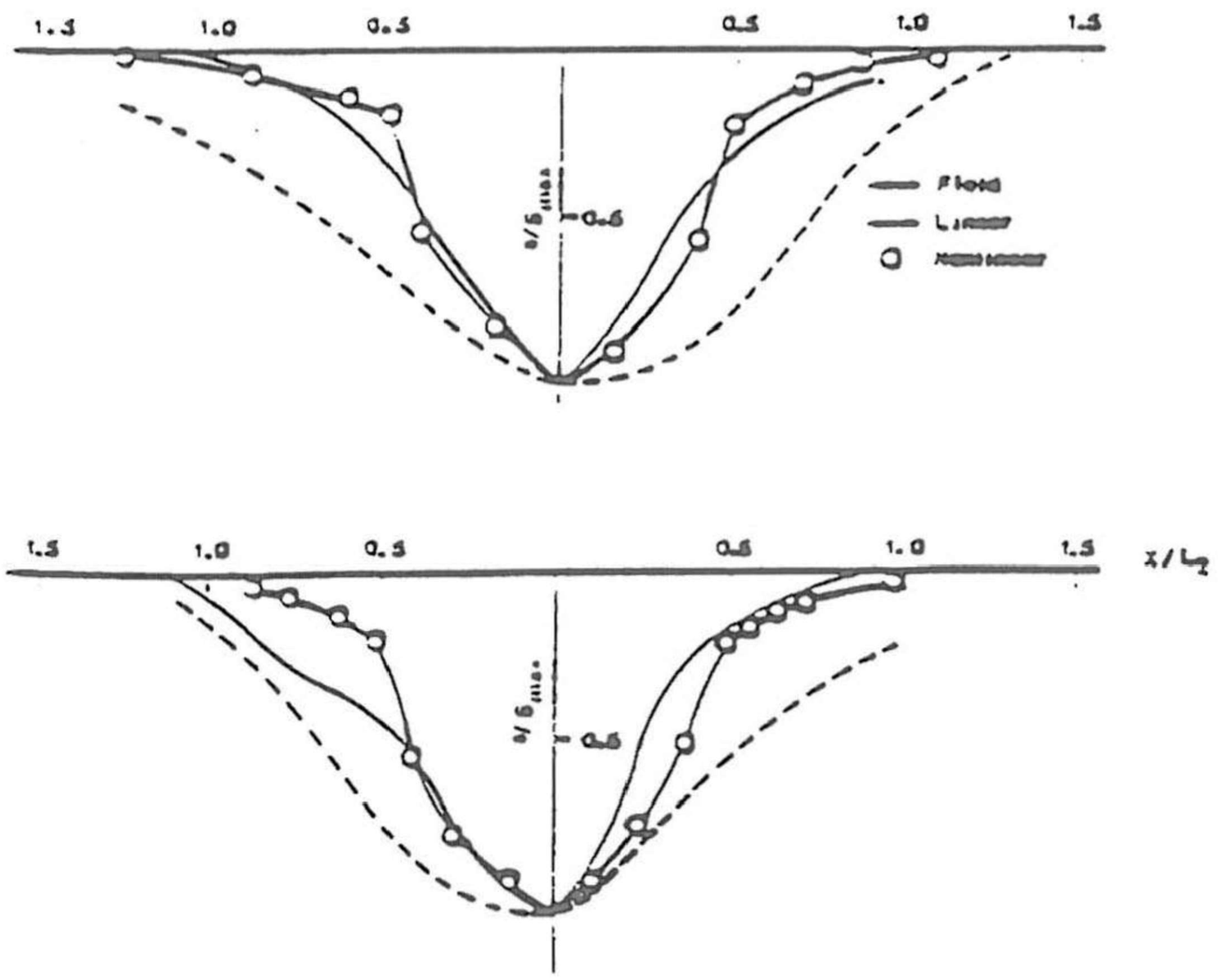

Fig. 12 Comparison of measured and predicted subsidence profiles by Siriwardane (1985).

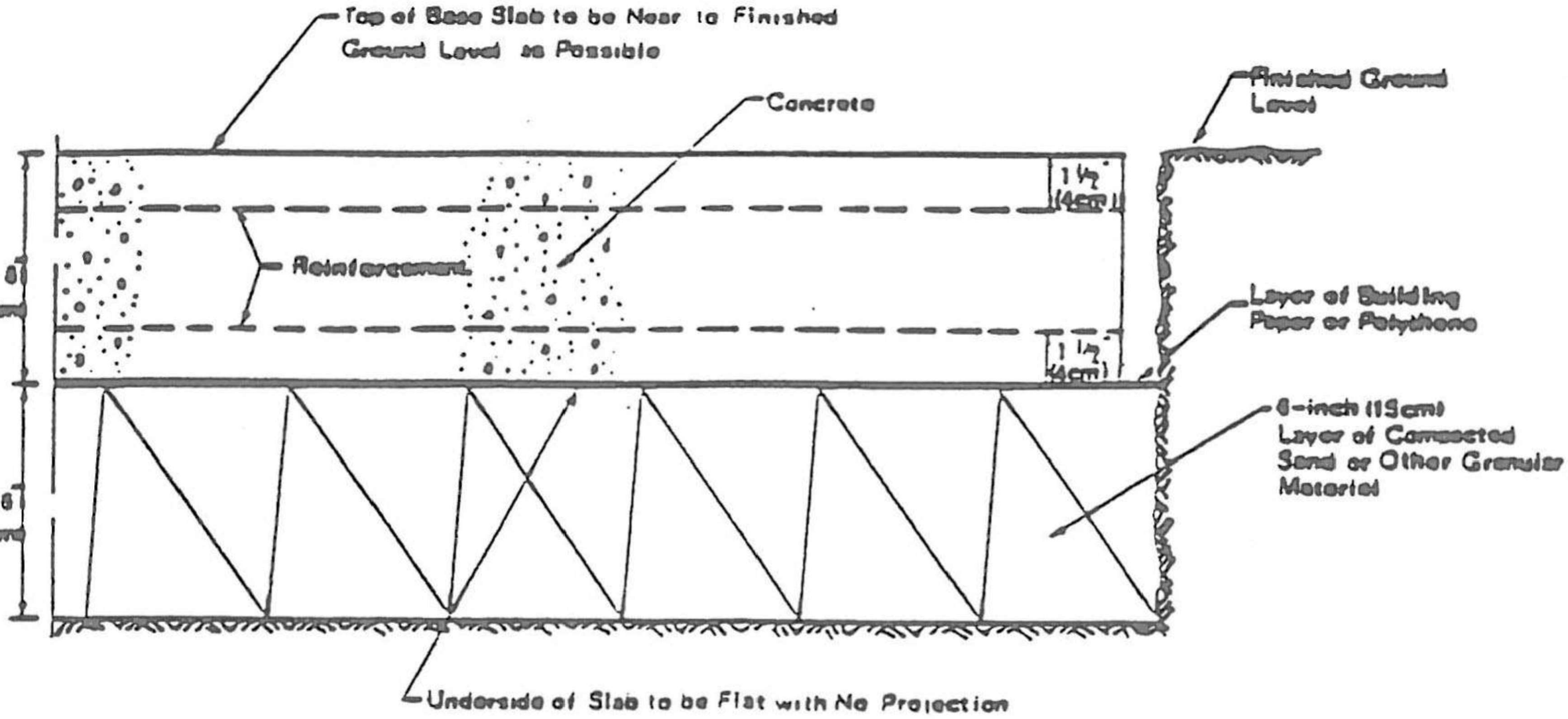

Fig. 13 Section of flexible slab foundation for small building (Baker, 1974).

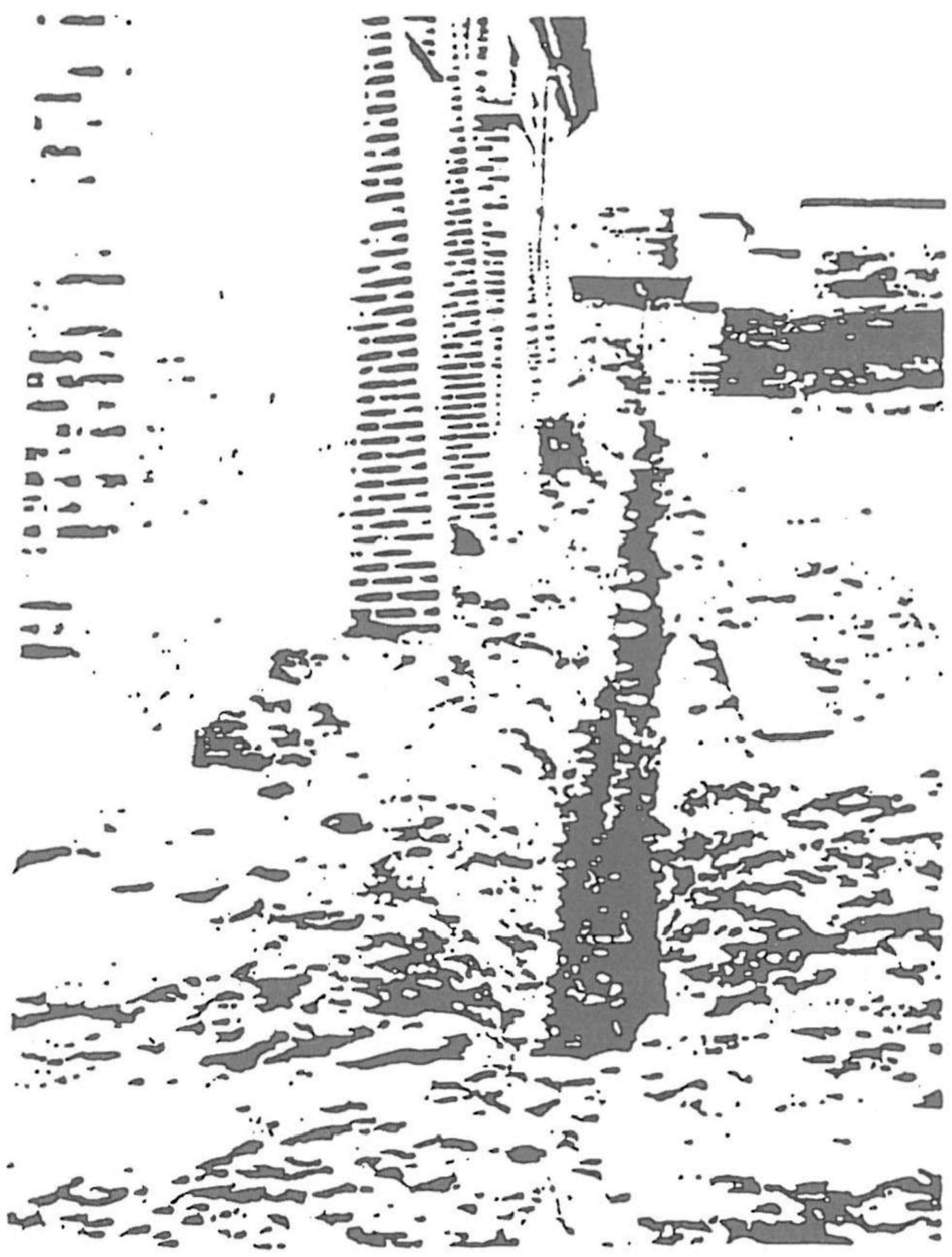

Fig. 14 Trenching around a building as a preventive measure.

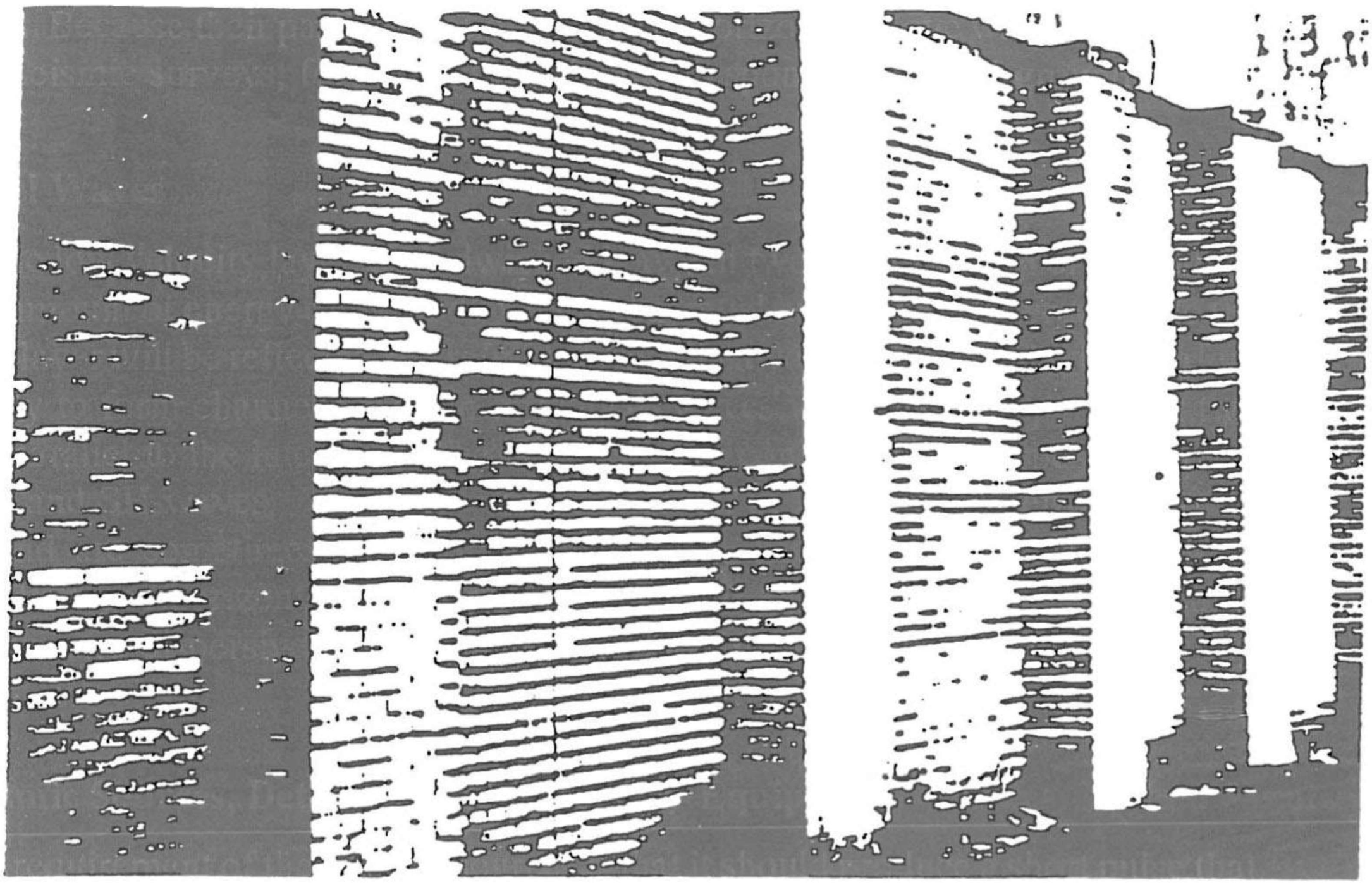

Fig. 15 Cutting through a brick wall as apreventive measure (Baker, 1974).

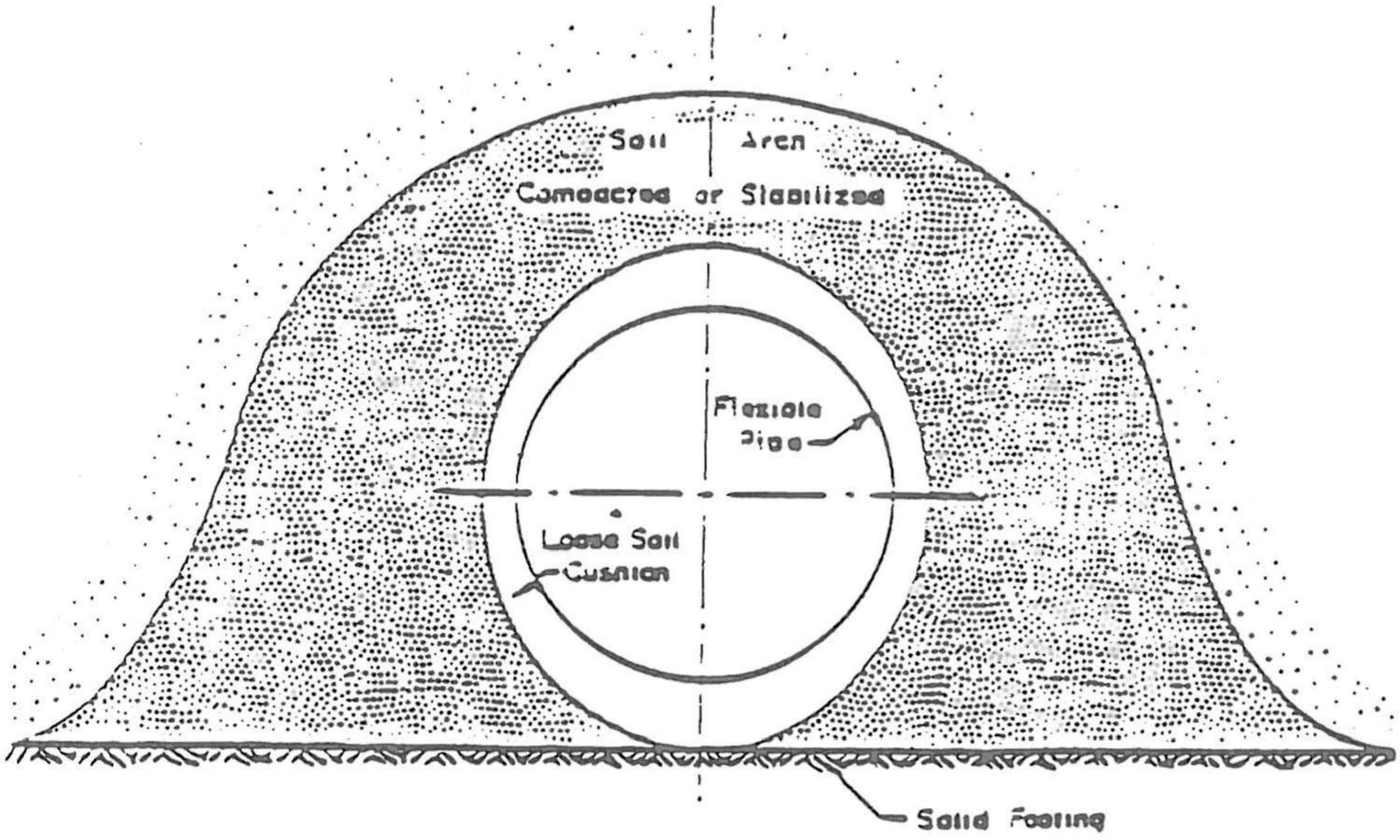

Fig. 16 Compacted soil arch with cushion to relieve stress in buried flexible pipe.

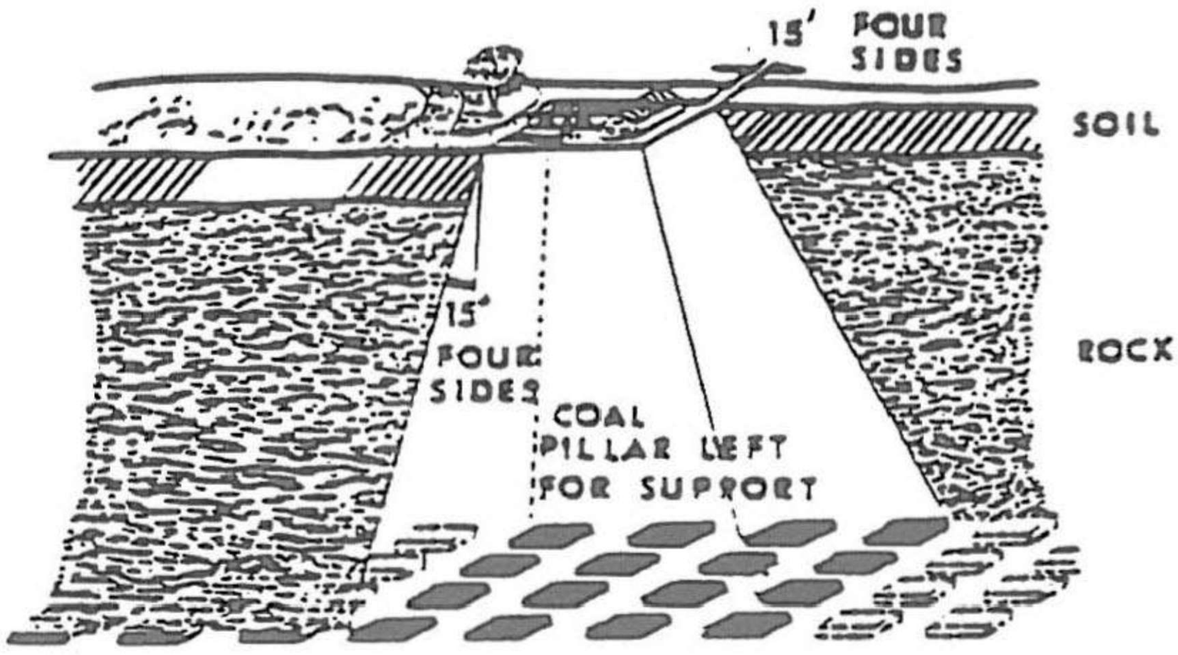

Fig. 17 Method of supporting structure (Gray and Meyers, 1970).

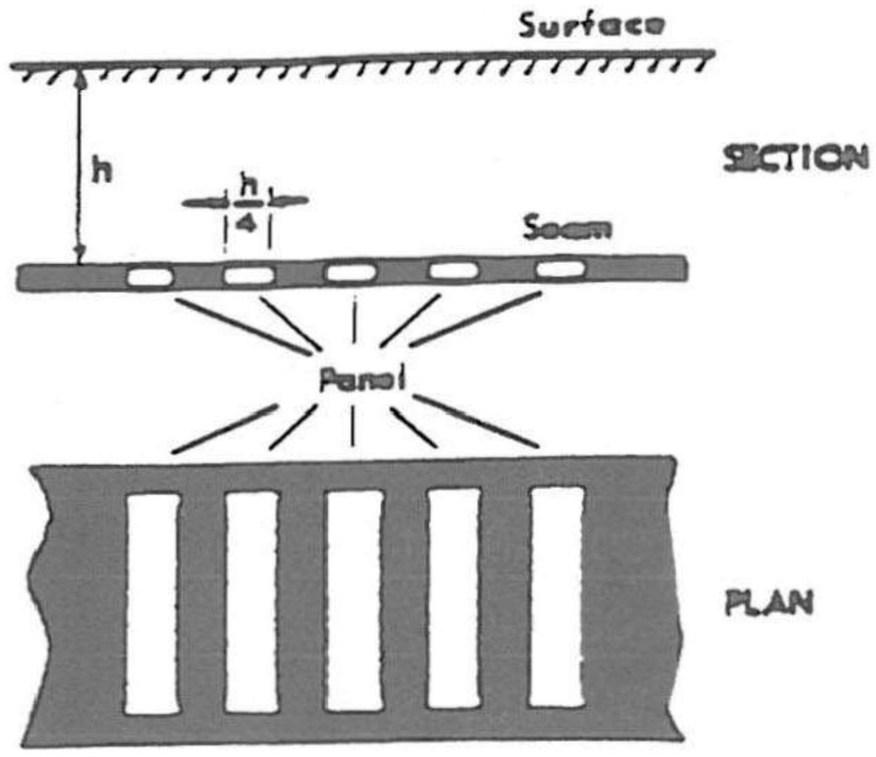

Fig. 18 Strip-pillared partial extraction system (Brauner, 1973a).

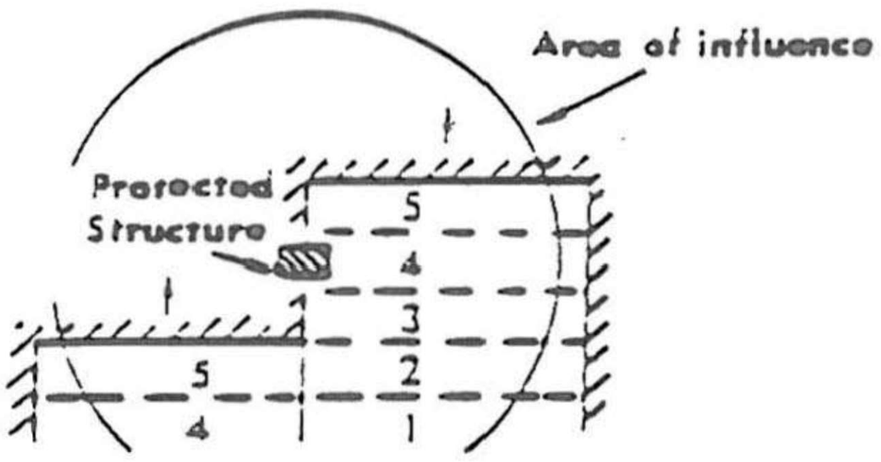

Fig. 19 Harmonic extraction with staggered faces (Brauner, 1973a).

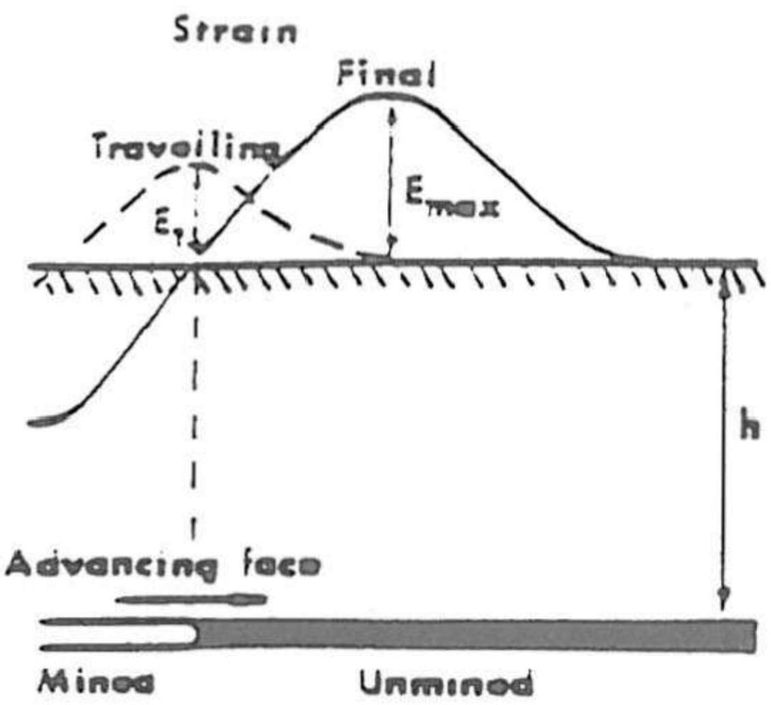

Fig. 20 Dynamic (traveling) strain is smaller than the final strain (Brauner, 1973b).

CONTENTS